# ThrustMIT's Project Vyom for the 10k Solid COTS category at the Spaceport America Cup 2018

**Technical Report** · January 2018

CITATION
1

READS
2,350

**12 authors**, including:

Nakul Gupta
Duke University
**1** PUBLICATION **1** CITATION
SEE PROFILE

Prashul Kumar
Indiana University Bloomington
**1** PUBLICATION **1** CITATION
SEE PROFILE

Saurabh Bagare
Indian Institute of Technology Bombay
**8** PUBLICATIONS **5** CITATIONS
SEE PROFILE

# ThrustMIT's Project Vyom for the 10k Solid COTS category at the Spaceport America Cup 2018

Team 06 Project Technical Report to the 2018 Spaceport America Cup

Nakul Gupta, Prashul Kumar, Vedang Kokil, Lokesh Kumar, Vishnu Teja Maddipatla, Amogh Govil, Saurabh Vijay Bagare, Mithil Bhuta, Rohith Warrier, Utkarsh Mehra, Ashish Samanta, Pavan Nimmagadda
*Manipal Institute of Technology, Manipal Academy of Higher Education, Manipal, Karnataka, 576104*

**ThrustMIT's debut at the Spaceport America Cup features it's first rocket designed to fly to 10,000 feet with a 4 kg payload, recoverable by a parachute. Powered by Aerotech's Commercial-Off-The-Shelf (COTS) solid-propellant M1845-P motor, the rocket shall be carrying a COTS as well as a student researched and developed flight computer named *Tron*. The apogee detection system is one unique characteristic of the launch vehicle, with a pitot tube being used in addition to a barometer to accurately detect apogee as well as eliminate chances of high speed recovery deployment. The rocket, named *Vyom*, features a fiberglass fuselage and fins and Aluminium 6061-T6 bulkheads, centering rings and motor block for added structural strength. The project was conceived in early 2016 with the aim to nurture rocketry as a hobby in India, and by competing at the Spaceport America Cup, the team will get a platform to share its knowledge as well as learn from fellow students from all around the world.**

## Nomenclature

| | | |
|---|---|---|
| $CG$ | = | Centre of Gravity |
| $CP$ | = | Centre of Pressure |
| $L$ | = | Lift |
| $D$ | = | Drag |
| $C_d$ | = | Coefficient of Drag |
| $C_l$ | = | Coefficient of Lift |
| $C_m$ | = | Moment Coefficient |
| $D$ | = | Diameter |
| $P_o$ | = | Total Pressure |
| $P$ | = | Absolute Pressure |
| $T$ | = | Temperature |
| $C_p$ | = | Coefficient of Pressure |
| $S_0$ | = | Nominal area |
| $D_0$ | = | Nominal diameter |
| $D_p$ | = | Projected Diameter |
| $D_R$ | = | Reefed Diameter |

## I. Introduction

ThrustMIT was conceived in February 2016 by a group of seven first-year engineering students studying at Manipal Institute of Technology, Karnataka, India, with the aim of promoting rocketry as a hobby in India, as well as competing against rocketry teams from all around the world at the Intercollegiate Rocket Engineering Competition. As of May 2018, the team has grown to thirty three members, with students from disciplines ranging from Mechanical Engineering, Information Technology, and Mechatronics to Aeronautical Engineering working together to design, build and fly model rockets as well as high power rockets for the annual Spaceport America Cup, starting 2018.

The 2018 team hierarchy back in India was as follows:

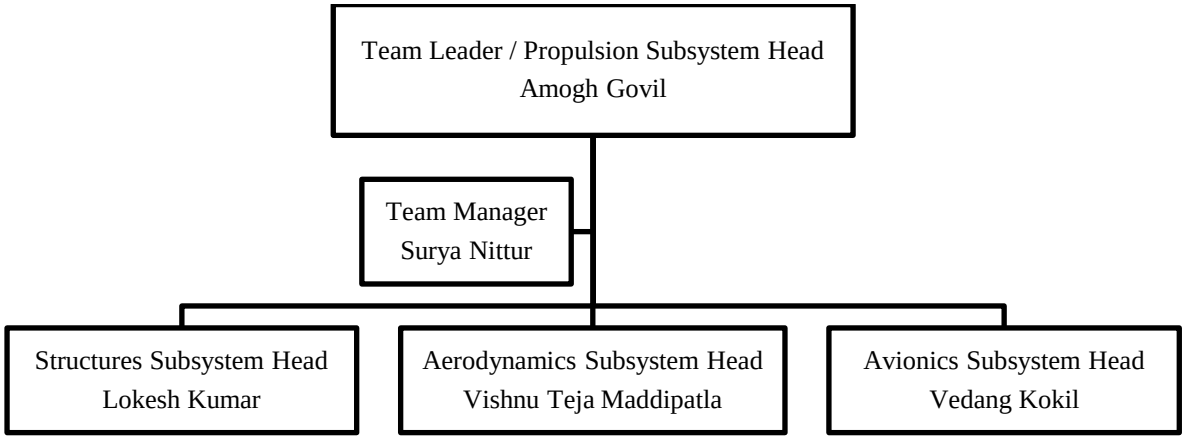


For the eleven member team attending the Spaceport America Cup 2018 in New Mexico, USA, the student team leadership will be as follows:

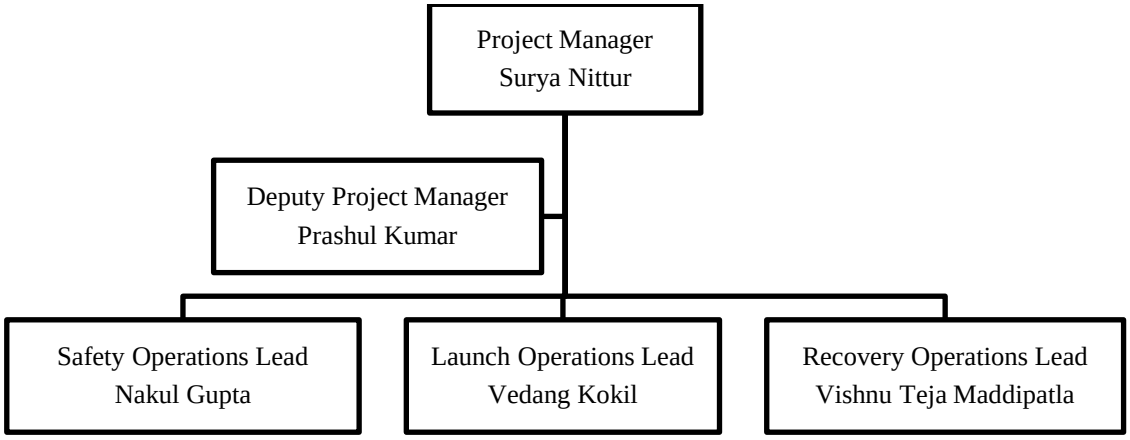


The team was funded by the university, Manipal Academy of Higher Education and was provided monetary as well as product and service support by its sponsors.

For its first competition, the team decided is going for a monocoque structure having a fiberglass body with aluminium structural components like bulkheads. The recovery system is pyrotechnic based with a 4kg boiler plate payload in the form of a 3U CubeSat. The avionics system has apogee detection and altitude logging, parachute ejection, range tracking, liftoff detection and data acquisition capabilities through the student researched and Developed (SRAD) flight computer, *Tron*, as well as a commercial flight computing system for dual redundancy. The motor used is Aerotech's M1845-P which will be wirelessly ignited. The unique feature of *Vyom* will be the use of a pitot tube for velocity prediction, which will cross-check velocity data gathered by the flight computer for greater accuracy and will reduce chances of high speed recovery deployment.

Having accumulated about 140,000 man hours of work before shipping its first rocket from India to the USA, the team hopes to make a mark in the second edition of the SA Cup, and share its knowledge and learn from other teams for continued participation and improvement in SA Cup editions in the coming years.

## II. System Architecture Overview

The launch vehicle airframe has a monocoque structure for its lightweight characteristics, ease of assembly and easy access to internal components. The fiberglass skin itself supports all bulkheads and centering rings, the structural analysis and feasibility of which is included further in the report. The various modules from top to bottom are:

1) Nose cone with integrated pitot tube system for improved apogee detection accuracy as well as eliminating chances of high speed recovery deployment.

2) Recovery bay with parachute ejection using pyrotechnics. The parachute itself will be reefed i.e., the drogue parachute will be deployed at apogee which will itself become the main parachute at 1500 feet when the reefing line is snapped.
3) Payload bay housing a 3U CubeSat payload weighing 4 kg.
4) Avionics bay housing *Tron*, the Student Researched And Developed (SRAD) flight computer, as well as a Commercial-Off-The-Shelf flight computer.
5) Motor bay with an aluminium 6061 and wood-polymer composite (WPC) motor block along with fins attached fiberglass flanges integrated to the fuselage.

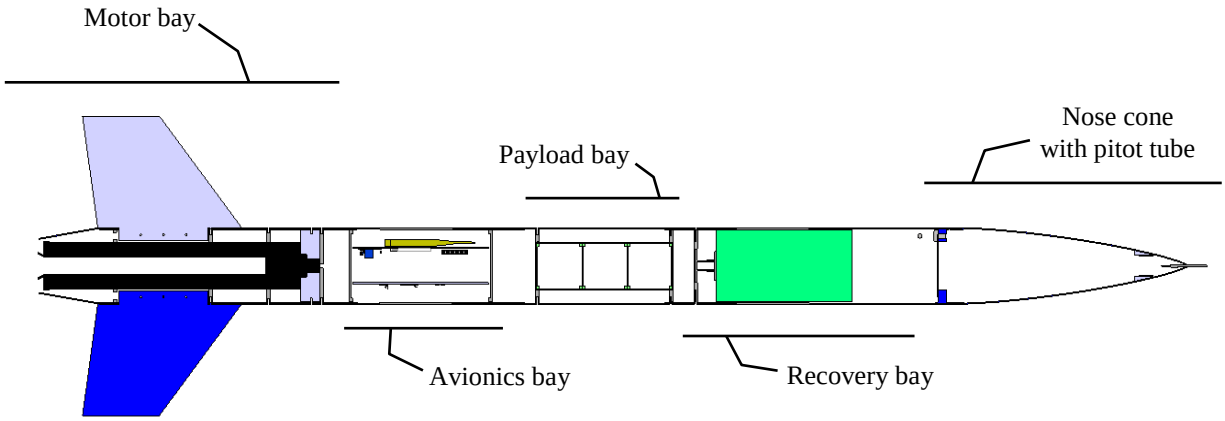


**Figure. Cut section view of Vyom**

### A. Propulsion Subsystem

The launch vehicle will be propelled by a Commercial-Off-The-Shelf (COTS) solid propellant motor, manufactured by Aerotech.

The motor model is M1845-P and uses an Ammonium Perchlorate Composite Propellant (APCP), also known as the 'Blue Thunder' propellant. This is because this propellant emanates a bright violet-blue flame on ignition, while producing minimal exhaust smoke. This fuel provides a more thrust than Aerotech's White Lightning or Black Jack motors of the same total impulse. The average thrust produced by this M class motor is 1675N and the peak thrust is 2434N. The total impulse produced by this motor is 8122Ns. The motor burns out in 4.73s and the impulse helps the rocket to travel for another 21s until it reaches the apogee. The thrust and impulse provided by this motor is sufficient to propel our 23.5 kg rocket to an altitude of 10,000ft.

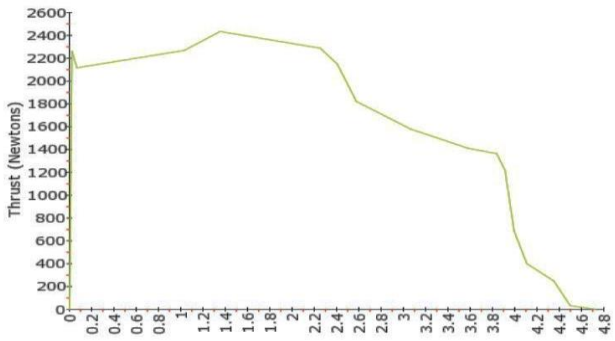


**Figure. Thrust curve for M1845-P motor**

The motor consists of a forward closure which holds the smoke charge cavity fitted in, which is the smoke charge insulator. The smoke charge gets ignited and then initiates combustion. This forward closure is attached to the motor through a forward seal disk through threads, supported by an O-ring. A composite liner is inserted in the motor which

acts as an insulator and also holds the three grain APCP propellant. The three grains of the propellant are separated by o-rings. The graphite nozzle is then inserted into the aft end of the motor case, with the nozzle flange seated against the liner assembly. Another o-ring is inserted to support the nozzle and then the aft closure is threaded into the motor case. The igniter is passed through the nozzle until it touches the smoke charge. The propellant weight is 3.718 kg while the total weight of the rocket motor, adding the fore and aft closures, is 6.682 kg.

The inner diameter of the motor bay is 156 mm and thus a motor of diameter 98 mm can be accommodated inside the rocket body. Three aluminum centering rings would prevent the motor axis from deviating from the rocket's vertical axis. To prevent the motor from going through the rocket body on ignition, an aluminum engine block is secured to the fuselage using fasteners as well as to the fore end of the motor using an eye-bolt. A wood-polymer composite bulkhead has been added below the aluminium engine block to act as an additional load bearing and supporting element.

To make sure that the engine block and centering rings do not fail on motor ignition due to sudden application of high load, we performed static structural analysis using ANSYS, to predict the extent of stress and deformation on the components.

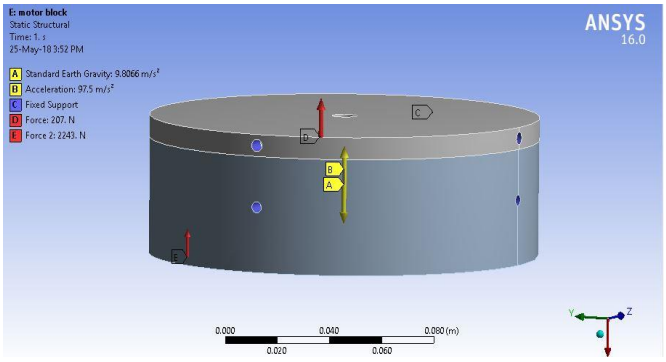


**Figure. Application of loads on the engine block.**

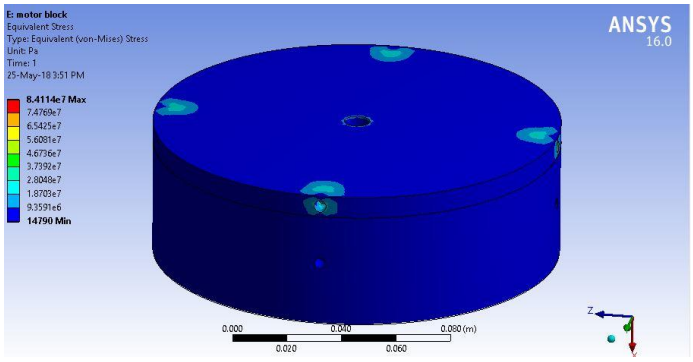


**Figure. Equivalent stress on the engine block.**

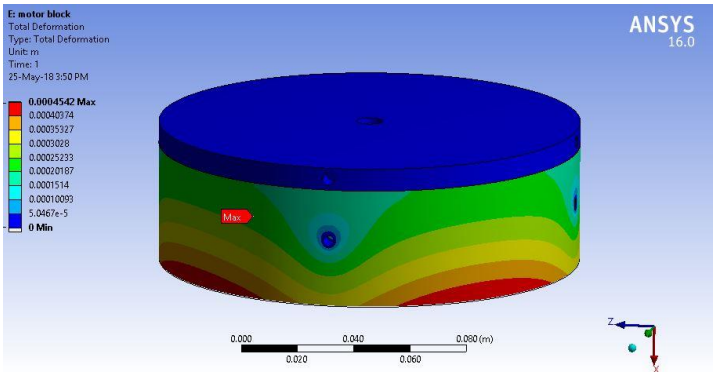


**Figure. Total deformation of the engine block.**

Four boundary conditions were considered during the analysis of the engine block.

a) The weight of the component.
b) The maximum instantaneous acceleration provided by the motor.
c) The fixed support by the fasteners through the four holes each on the aluminium and wood-polymer composite (WPC) engine block.
d) The maximum instantaneous force exerted by the motor on the engine block (both on WPC and aluminium).

The maximum force and acceleration have been applied at the same time on the engine block as a worst-case scenario for maximum load on the engine block.

As can be seen from Fig. 2, the maximum stress encountered by the engine block is about 84 MPa in the vicinity of the holes for fastening the bulkhead to the fuselage. Since the tensile yield strength of aluminium 6061-T6 is about 276 MPa, we get a factor of safety of over 3, indicating a reasonably safe design.

The deformation in Fig. 3 is shown to be about 0.45 mm, however, this large deformation is expected to be on the WPC bulkhead, not on the aluminium one. Considering the fact that the WPC bulkhead is not the primary load bearing member, and acts primarily as a cushion, this magnitude of deformation is not critical and is therefore, acceptable.

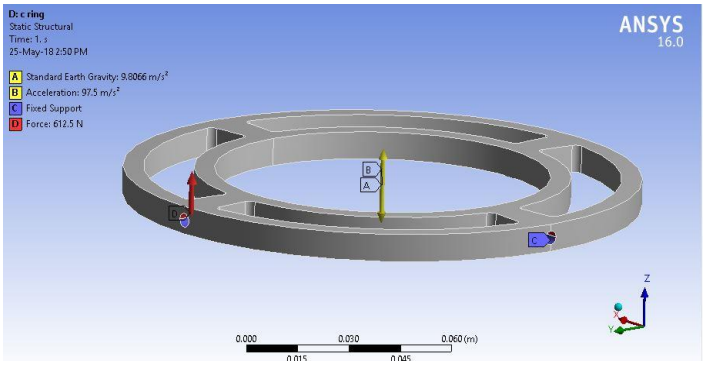


**Figure. Application of loads on a centering ring.**

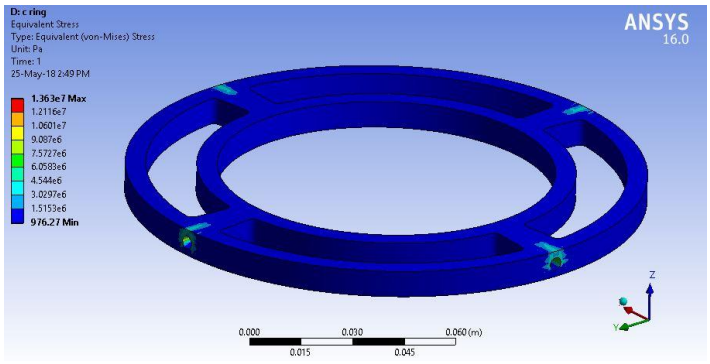


**Figure. Equivalent stress on the centering ring.**

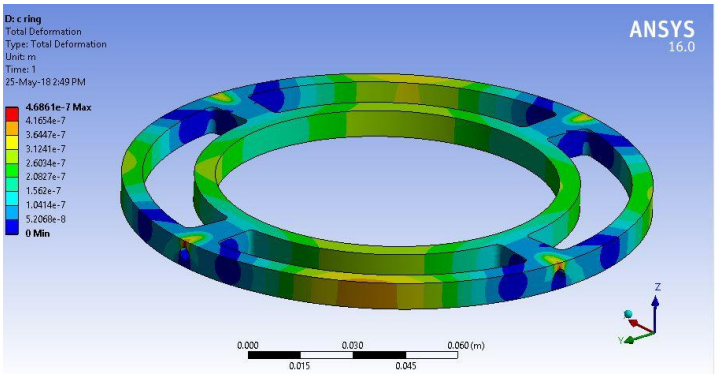


**Figure. Total deformation of a centering ring.**

During the analysis of a centering ring, we realized that there are no direct forces from the motor to the centering ring, except if the motor is slightly misaligned and transfers some load due to contact. The primary load on the centering rings are be due to the flow of force from the motor to the motor block to the fuselage and finally to the centering ring. This would mean the effect of thrust would be on the upper half of the holes made for fastening. Consequently, the stress and deformation expected to be on the centering ring is about 14 MPa and 0.0005 mm respectively, well within the safe limits.

## B. Avionics Subsystem

The team has built its own SRAD flight computer, named *TRON*.

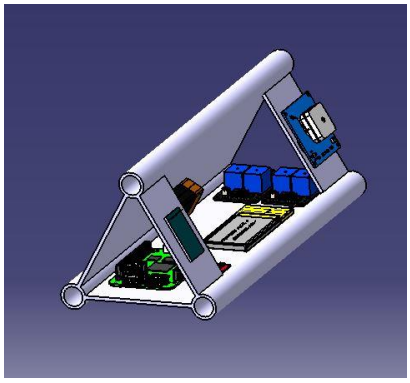

**a)**

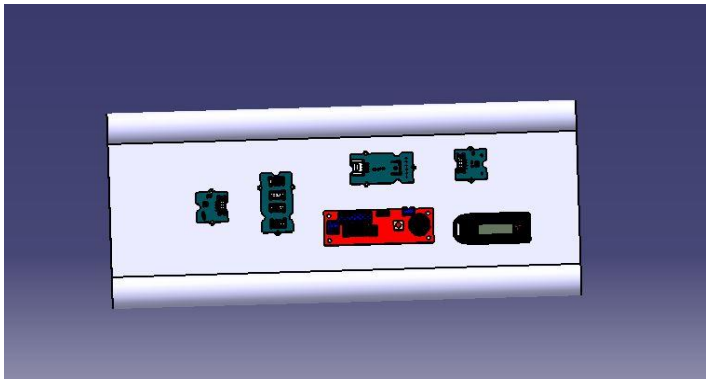

**b)**

**Figure. Avionics bay**

The electronics component mount is triangular prism shaped with 16mm cylindrical slots on the three edges along the length. The triangular shape was chosen as it provides the most stability and it gives us sufficient space to place all the sensors and micro-controllers. 3 aluminum rods pass through the slots to support the mount and minimize vibrations.

Figure 1 shows a layout of the avionics bay. As in Fig. 1, we use the Beagle Bone Green as our main controller. It contains an AM335x 1GHz ARM cortexA8 processor with 512MB DDR RAM and 4GB 8-bit eMMC on-board flash memory. It comes with a pre-installed OS which makes it reliable to use. We chose Beagle Bone Green over Beagle Bone Black because of its unique modifications and applications. It has a groove connector which makes it user friendly by allowing a wide variety of groove sensor family. We use a combination of different sensors, all of them from the groove sensor family. The sensors used are:

1) BMP280, a barometric pressure sensor with a range of 300 – 1100 hpa and an accuracy of (+-) 1.0 hpa. It also has a temperature measurement ranging from -40$^{o}$C to 85$^{o}$C.
2) LSM6DS3, a 6-axis gyroscope and accelerometer with accelerometer sensitivity ranging from (+-) 2g to (+-) 16g, sufficient to capture the initial thrust. The gyroscope can measure the angular rate at 125, 250, 500, 1000, 2000 DPS (degrees per second).

The barometer, which was a crucial part of *TRON*, was calibrated using a subsonic wind tunnel. After a number of tests, we finalized the port hole dimensions and the calibration constant. A static calibration for the fusion of accelerometer and gyroscope was achieved by attaching the sensor to a wooden plank and matching the true tilt against the sensor tilt. The calibration constant for roll, pitch and yaw were then finalized. The accelerometer was calibrated to read out 1g and detect liftoff.

The magnetometer in the rocket is used for data acquisition of magnetic field at high altitudes.

The avionics system is required to perform motor ignition, apogee detection and altitude logging, parachute ejection, range tracking, data acquisition and liftoff detection.

1) **Motor ignition**: A wireless ignition system having two components, a transmitter and a receiver, has been developed. The wireless communication will be carried out using HC-12, a wireless serial communication module having a range of 1000m. The transmitter will have three switches, one for the main power supply, one for arming and one for the final ignition. The receiver on the other side will have an electronically controlled switch which will supply the ignition charge when it catches a specific array of characters from the transmitter.
2) **Apogee detection and altitude logging**: We have developed a unique technique for apogee detection which will involve a combination of pressure readings captured by a barometer in *Tron* with the readings from the pitot tube system.
    a) **Pitot system**: Velocity prediction using a pitot tube has been a common practice in aerospace, especially in aircrafts. Pitot tube works on the principle of Bernoulli theorem for streamline flow of fluids. This is done by calculating the pressure difference by using two barometers, one for the static pressure and the other, for the dynamic pressure. The difference of these two quantities is known as the dynamic pressure which is then used to calculate the velocity of the rocket.

    To create the total pressure port, a hole has been drilled in the nosecone tip to accommodate the insertion of a pitot tube of 4mm diameter. Vinyl tubes have been used to connect the port holes of the sensor the pitot tube. While assembling the pitot system, it should be ensured that the static port is not on the angled surface of the nosecone, instead, it is on the cylindrical portion of the fuselage or at the base of the nosecone.

    Multiple wind tunnel tests were carried out to check the accuracy of the pitot system and for the calibration of the sensor**.** An accuracy of about 3 m/s was achieved.

    b) **Apogee detection condition:** We have two phases of apogee detection. The first phase consists of getting readings from our barometer BMP280 and passing them through low pass filters to smoothen them out .Then we use the scientific fact that as altitude increases, the pressure decreases, to detect the apogee by sampling values at regular intervals. Once apogee is detected in this phase, we check the pitot readings and if they are within a predefined velocity range only then apogee deemed to be accurately detected. The pitot system is present to remove any false apogee detections the first phase might calculate, and it also helps in preventing any chance of high speed recovery deployment.
3) **Parachute ejection**: Once the apogee is detected, the next task is to deploy the drogue chute to reduce drift and stabilize the rocket at 10,000 feet. This is done through an electronically controlled switch. As soon as

the apogee is detected the micro-controller activates the switch. A 7.4V 2S 1000 mAh battery supplies about 3.5 A of current to a nichrome wire which heats up, igniting the black power. The black powder is filled inside an aluminium cylinder known as a pyro container which then creates a suitable pressure which pushes out the nosecone and the parachute.

4) **Range tracking**: After the parachute is deployed, the wind may take the rocket far away from the expected landing. In order to keep a track of the rocket, we need to have some tracking mechanism. Generally, rocketeers use the BigRedBee GPS modules to get the location of the rocket. The BigRedBee GPS modules come with an RF module so that it can transmit the location of the rocket at certain time intervals. But the $400 price tag on it is not worth the investment. So we decided to go with the Adafruit Ultimate GPS module. It is a low powered, effective and compact location provider. The team has developed a live telemetry system for real time plot of the rocket trajectory. For the wireless transmission over a distance of 3 km we decided to go with the standard Xbee S2 PRO 9000 MHz which will provide us a range of 6 km with a standard 2.1 dipole antenna. All the required data for the trajectory plot is collected in the micro-controller and then passed on to the Xbee module, which then sends it over to the receiver system. The receiver system sends it to a laptop which has a customized plotting software.

**5) Liftoff Detection:** Without knowing when liftoff occurs, it would be futile to detect apogee, hence liftoff detection enables the apogee detection module. We have used two systems independent of each other to detect liftoff. LSM6DS3 is a sensor that contains a combination of an accelerometer and a gyroscope. The accelerometer is used to detect changes in acceleration exceeding 4g to detect liftoff. If this system fails, there is a backup barometric system which is used to detect liftoff. Initial acceleration in the rocket would be high due to which there will be a significant change in pressure which is used to detect liftoff.

**6) Data Acquisition:** We have an SD card connected to the beagle bone that logs all the data given out by the sensors for future analysis. We shall also transmit live data to the ground station in case the data in SD card onboard becomes irrecoverable so that the data stays safe. At the ground station, the data received will be plotted and saved simultaneously for future use.

**7) Qt based plotter:** The plotter is based on C++ for relatively faster execution while keeping in consideration practical aspects like community support and available open-source libraries. It uses Qt, a powerful C++ SDK that provides support for complicated Graphical User Interface (GUI) (and corresponding interactions) and has a wide community. The QCustomPlot library was used for plotting. Some features included in the software are:

a) The plotter supports plotting of live data stream from a serial port, or a text file.
b) According to the requirements, 2 modes for plotting are supported. One graph per plot or three graphs per plot which have been designed by us.
c) When using the serial port as an input, *files are created and all received data is stored automatically*, which can be directly plotted from after.
d) Dynamically changing the maximum number of data points visible in a graph at any time is supported.
e) Scrolling through the graph is allowed to study the graph at an earlier time.
f) Options like top padding and bottom padding are present to control the range over which data is viewed.

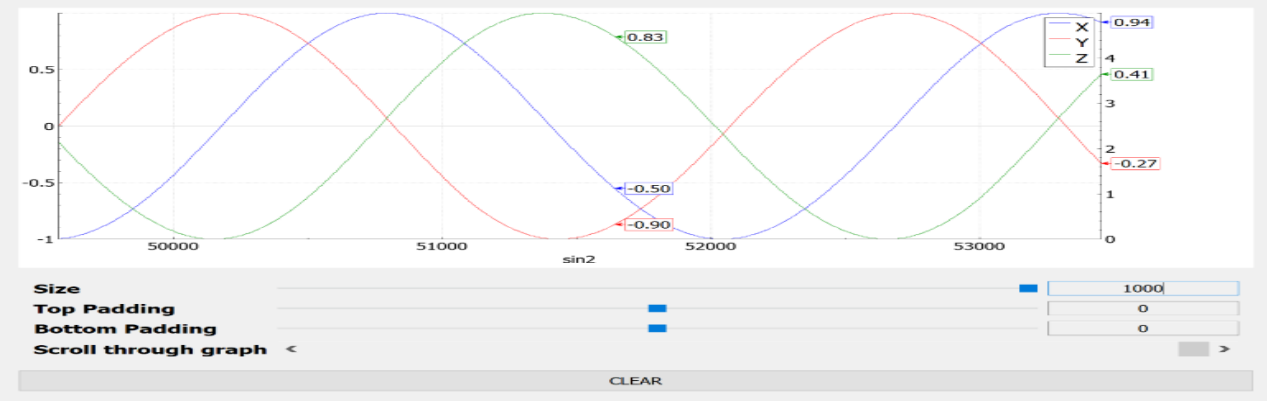


**Figure. GUI and plotter**

The team has developed a mathematical model for rocket dynamics using MATLAB. This is to simulate the environmental conditions throughout the rocket trajectory i.e., the rocket flight is simulated using MATLAB.

The simulink model thus developed is

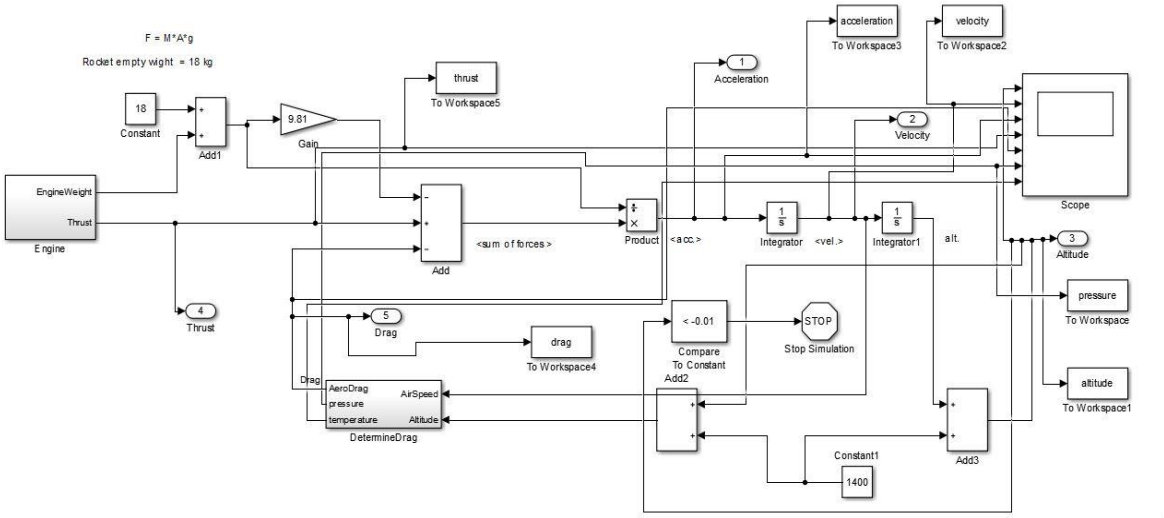


**Figure. MATLAB Simulink model for rocket flight simulation**

The Simulink model has two subsystems, one to determine drag and one for engine block.

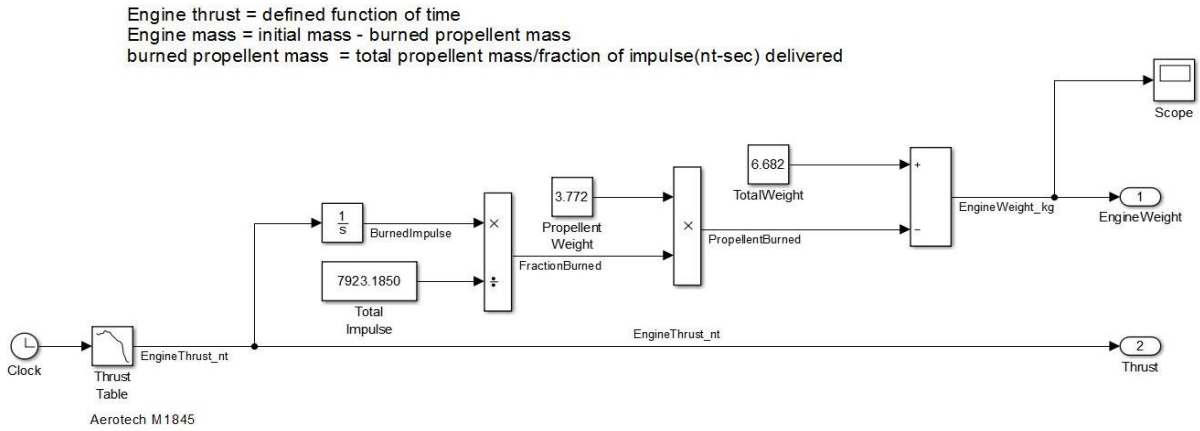


**Figure. Engine block**

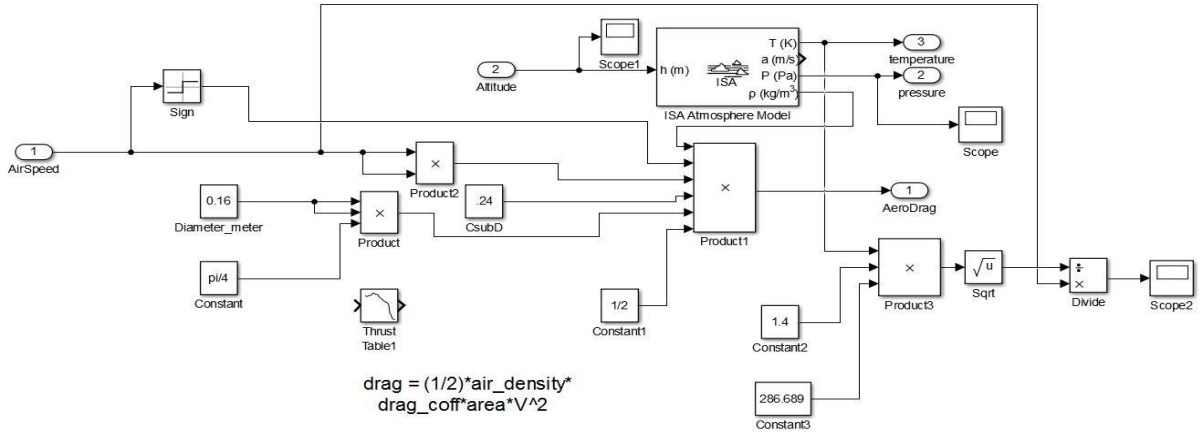


**Figure. Determine Drag Block**

The results of this model were:

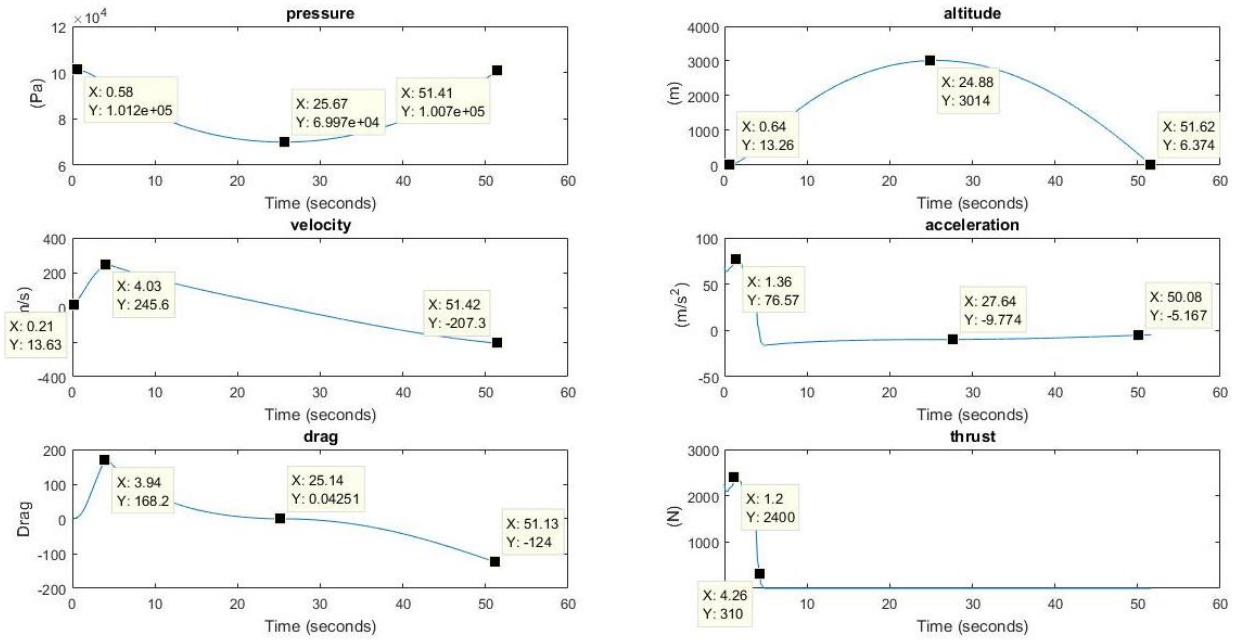


**Figure. Results of the Apogee Prediction Model**

### C. Aero-structures Subsystem

The following softwares were used for design and simulation of Vyom.

- *CATIA*- For Computer Aided Design of rocket components.
- *SolidWorks*- Design and modelling of payload and its components. Also used for simulation.
- *OpenRocket*- Open source software for 2D design plan of rocket and to get an estimate of arrangement of internal components inside the fuselage. This software was also effectively used to get simulation results and to get geometrical understanding of the design.
- *MATLAB*- Code to generate the 1/8$^{th}$ portion of the in-house designed reefing parachute.
- *ANSYS*- Fluent and static structural workbenches used to obtain the Computational Fluid Dynamics and Stress Analysis results.

A typical flight of a model rocket can be characterized by the four phases:

1. *Launch*: The model rocket is launched from a vertical launch rod/rail.
2. *Powered flight:* The motor accelerates the rocket during the powered flight period.
3. *Coasting flight:* The rocket coasts freely until approximately at its apogee.
4. *Recovery:* The recovery device opens and the rocket descends slowly to the ground.

**Design**

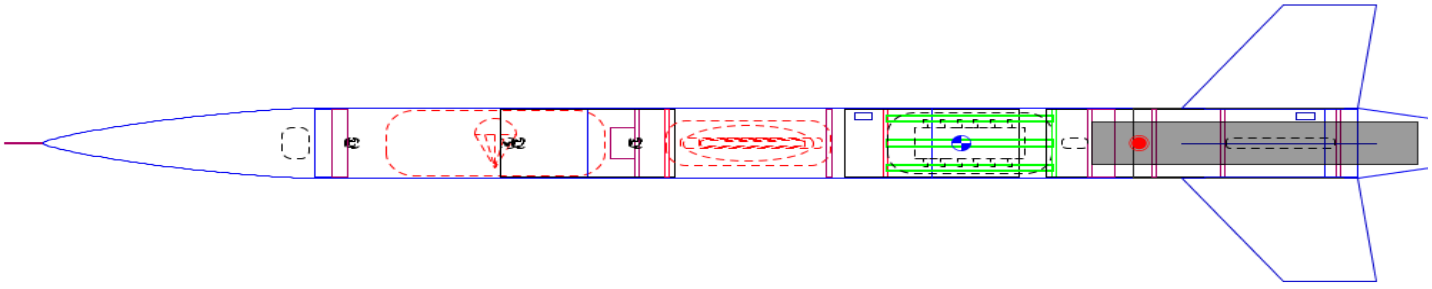

**Figure. OpenRocket model of *Vyom***

The outer design of Vyom is a 4-fin design (Crusiform) with a modular monocoque structure. The modular design is to allow calibration of the avionics.

**Aerodynamic Properties of Rocket**

A model rocket encounters three basic forces during its flight: thrust from the motor, gravity, and aerodynamic forces. When the force due to gravity on each component is summed up, the gravitational force can be seen as a single force originating from the centre of gravity (CG). A homogeneous gravitational field does not generate any angular moment on a body relative to the CG. Calculating the effect of gravitational force is therefore a simple matter of determining the total mass and CG of the rocket.

Aerodynamic forces, on the other hand, produce both net forces and angular moments. To determine the effect of the aerodynamic forces on the rocket, the total force and moment must be calculated relative to some reference point.

**Major aerodynamic elements:**

**a) Nosecone**

At subsonic speeds the pressure drag of streamlined nose cones is significantly smaller than the skin friction drag. In fact, suitable shapes may even yield negative pressure drag coefficients, producing a slight reduction in drag. From the data that is available on various journals and databases, it can be concluded that there are various types of nose cone designs like ogive, parabolic, conical, bi-conical etc.

From OpenRocket simulations and datasheets, the team decided to go with Van-Karman LD Haack series nosecone where LD stands for Length-Diameter, which means that for a given length and diameter on a 2D plan, this design will experience minimum drag.

Von-Karman or Haack series nosecones are not obtained by geometric figures, but are derived for the purpose of minimizing drag. MATLAB code for generating LD Haack nosecone is as shown:

```
clc
clear all
r=input('Enter radius: ');
l=input('Enter length: ');
axis equal

x=0:0.1:l;

k=0;

t=acos(1-(2*x)/l);
y=(r/sqrt(pi)).*sqrt(t-
(0.5*sin(2*t))+(k.*sin(t.^3)));
plot(x,y)
%[X,Y,Z] = cylinder(y);
%surf(X,Y,Z,'edgecolor','none'), axis square;
```

**Figure . MATLAB code for Haack nosecone.**

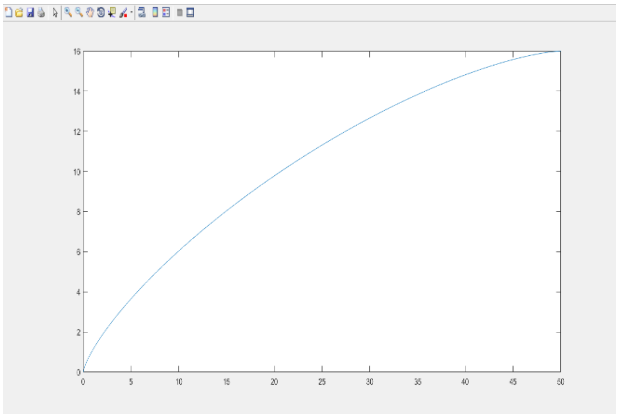

**Figure. 2D nosecone profile for *Vyom***

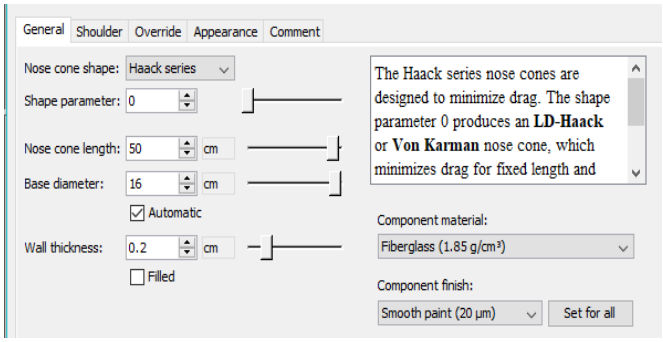


**Figure . OpenRocket parameters for nose cone**

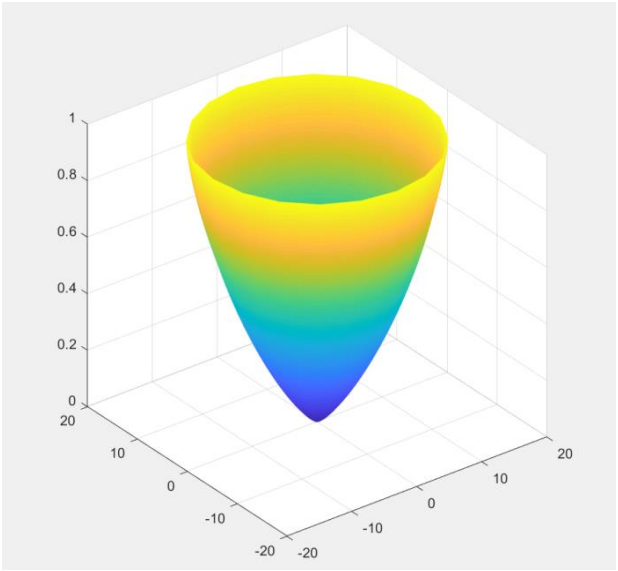

**Figure . 3D profile of nose cone based on MATLAB**

**b) Body Tube**

The centre of gravity is 168 cm from the tip of the nosecone and centre of pressure is at 201 cm. The MATLAB code for barrowman equation is as given below:

```
clc
clear all

Cnn=2;
Ln= input('Enter length of the nose: ');
k=input('Press 1 for conical and 2 for ogive: ');
if(k==1)
   Xn=0.666*Ln;
else
   Xn=0.466*Ln;
end

n=input('Enter number of fins: ');

fprintf('Fin Terms: \n');

s=input('Enter fin height: \n');
d=input('Enter diameter at the base of the nose: \n');
Lf=input('Enter fin mid-chord length: \n');
Cr=input('Enter fin root chord: \n');
Ct=input('Enter fin tip chord: \n');
r=input('Enter radius at aft end of fuselage: \n');

Cnf=(1+r/(s+r))*(4*n*(s/d)^2/(1+sqrt(1+(2*Lf/(Cr+Ct))^2)));

Xb=input('Enter distance from nose tip to fin root chord leading edge: \n');
Xr=input('Enter distance between fin root leading edge and fin tip leading edge parallel to body: \n');

Xf=Xb+(Xr/3)*(Cr+2*Ct)/(Cr+Ct)+(1/6)*(Cr+Ct-Cr*Ct/(Cr+Ct));

fprintf('Finding centre of pressure ');
Cnr=Cnn+Cnf;

X=(Cnn*Xn+Cnf*Xf)/Cnr;

fprintf('The Position of CP from nose tip is: ');
disp(X);
```

**Figure. MATLAB code for Barrowman equation**

**c) Fins**

Based on our research on rocket fin design, we concluded that for stability of a rocket, minimum three fins were required. The design of *Vyom* employs 4 fins on a freeform plan design. The simulation is done on OpenRocket and ANSYS and results show that the design yields a stability calibre of 2.04 at 0.10 M.

The range of static stability calibre ranges from 1.6-2.95 through the flight.

The detailed plan of single fin is given below:

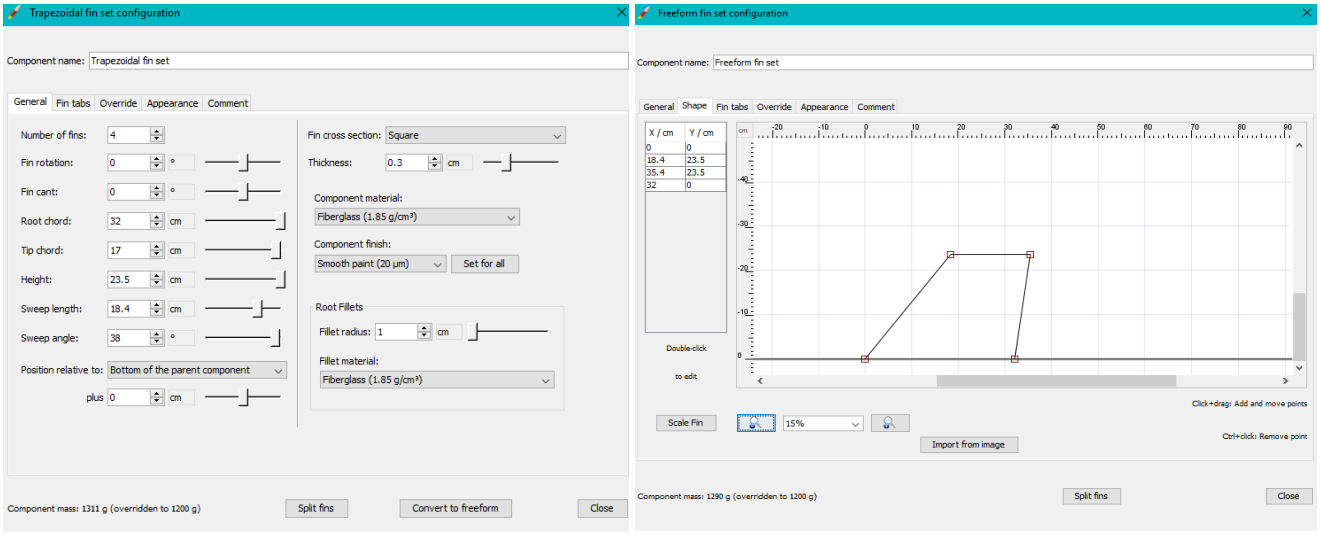


a) b)

**Figure. Detailed plan for fins for Vyom**

Some of the OpenRocket simulations results are as follows:

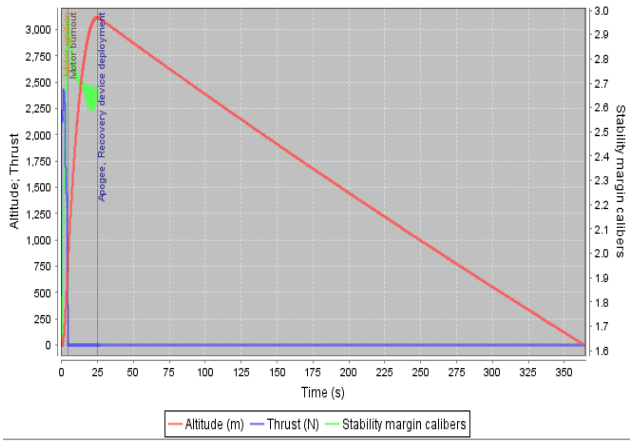


**Figure. Altitude, thrust and stability margin (calibers) vs time**

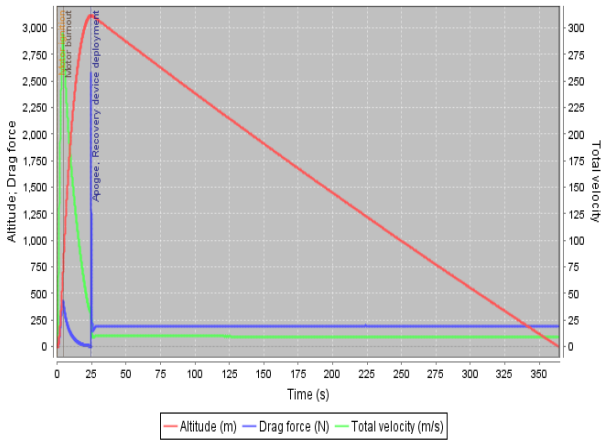


**Figure. Altitude, drag and total velocity vs time**

### d) Boat Tail

There is a popular concept in aeronautics known as Bluff Body Aerodynamics. This means that all blunt bodies experience a sudden increase in dynamic pressure (adverse pressure gradient) which results in a phenomenon called as wake. They are hazy irregular airflow patterns seen commonly in day to day objects. This wake results in an increase in drag called as wake drag.

This drag is an unnecessary cause of decrease in velocity and can be minimized by the presence of a structural element called as 'Boat Tail.' This boat tail ensures that the wake does not affect the primary aerodynamics of the body. In this case, the fuselage acts as a blunt body. The boat tail is the last section of the rocket guarding the motor at the rear end.

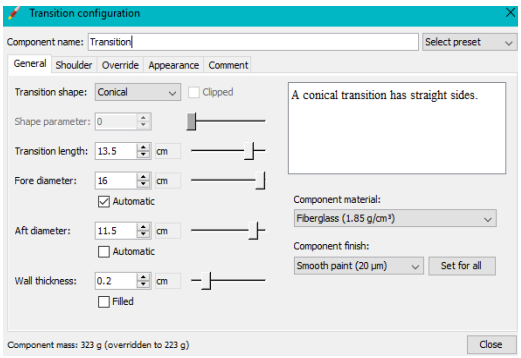


**Figure. Design parameters for the boat tail**

### e) Pitot-Tube

A pitot tube in subsonic flow measures the local total pressure $p_0$. Together with a measurement of the static pressure p, the Mach number can be computed from the $p_0/p$ ratio.

**Analysis of strength of aero-structures to sustain loads in different stages of flight**

**a) Strength against shear load on fiberglass composite body when the recovery pyrotechnique is fired**

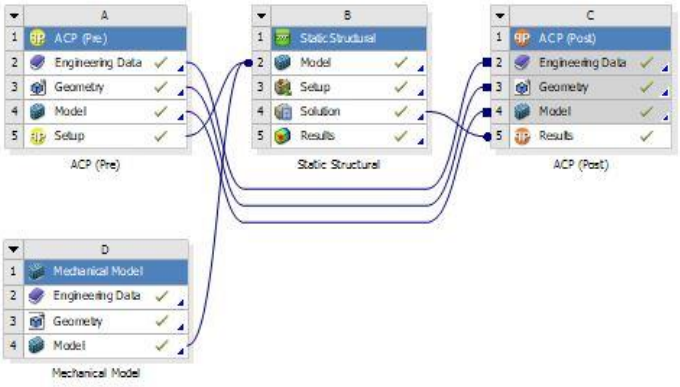


**Figure. Simulation tree for analysis of fiberglass body before and after the black powder for recovery is fired.**

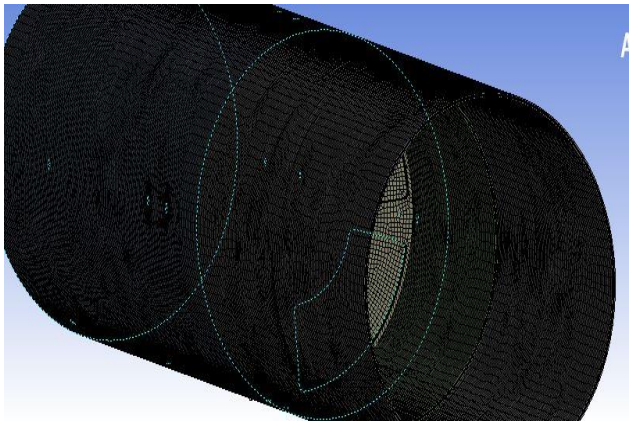

**Figure. Body tube mesh for analysis.**

The following boundary conditions were applied for the simulation to determine the effect of pyro on the body:

i. Pressure: 10 psi on recovery bulkhead
ii. Fixed supports: Holes on bulkhead for fastening to body
iii. Weight

At the apogee, there would be no vertical acceleration except the acceleration due to gravity.

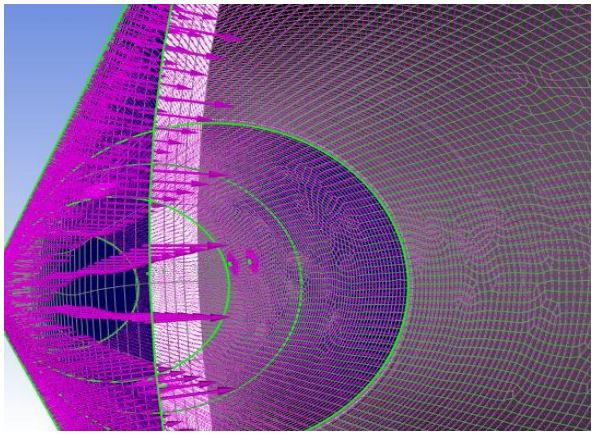

**Figure. Orientation of the fabric in the body tube**

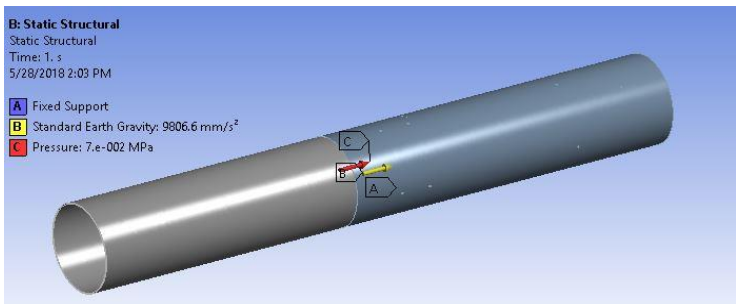


**Figure. Boundary condition as applied on the body tube**

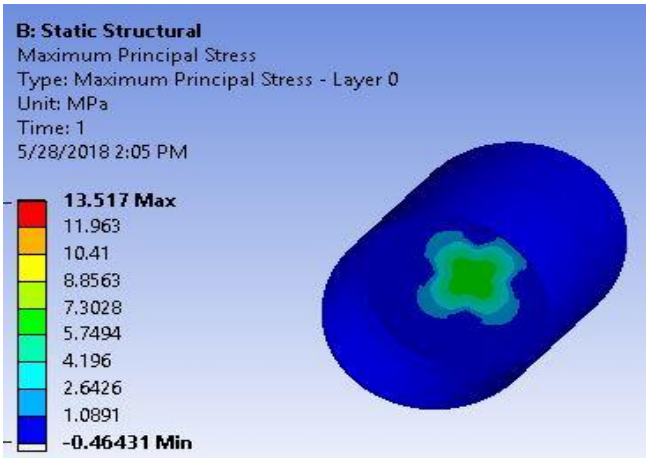


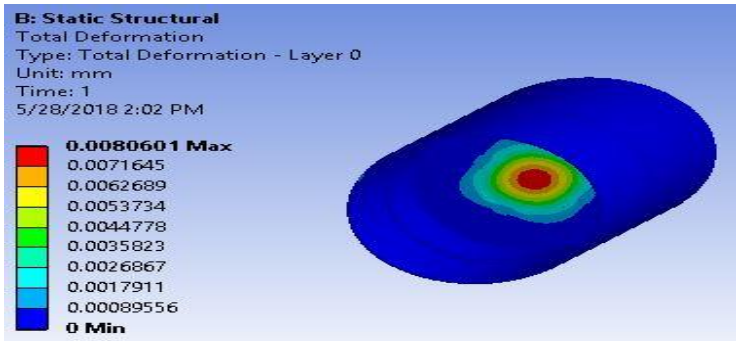


**Figure. Total deformation experienced by body.**

**Figure. Maximum principal stress experienced by the body.**

### b) Analysis of recovery bulkhead when pyro is ignited

Next, we carried out static structural analysis of the bulkhead used in the recovery system to hold the pyro container in place. The boundary conditions applied were:

i. Weight of the bulkhead
ii. Maximum acceleration of the rocket
iii. Pressure of 10 psi (68950 Pa) developed inside the pyro container.
iv. Fixed support on the four holes for fastening
v. Maximum thrust by the motor

Though the maximum acceleration and thrust do not act at the same time as the pressure due to pyro firing, it is assumed to occur at the same time just as a worst case scenario of all loads acting at once.

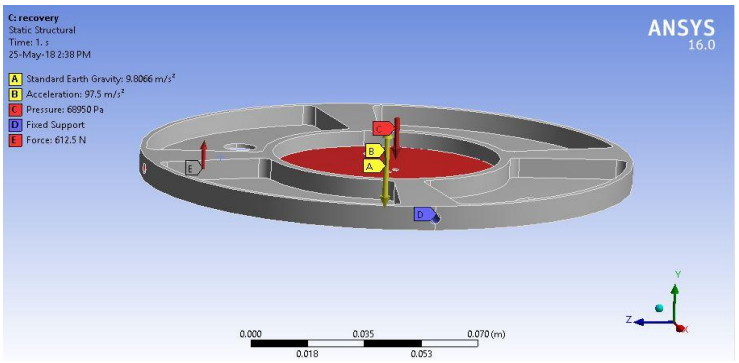


**Figure. Application of loads and supports on bulkhead for recovery.**

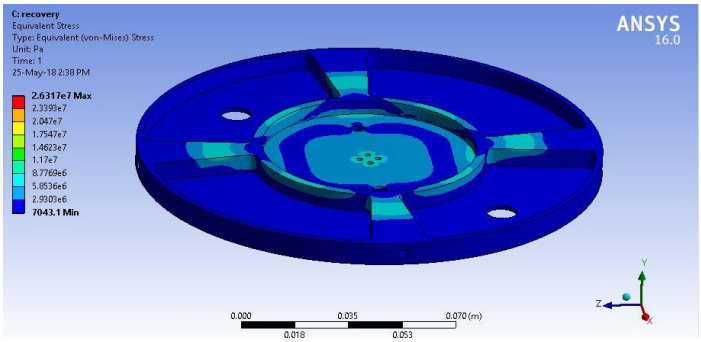


**Figure. The equivalent stress experienced by the bulkhead.** The maximum stress came out to be about 26 MPa, giving a factor of safety of over 10.5, indicating a very conservative design.

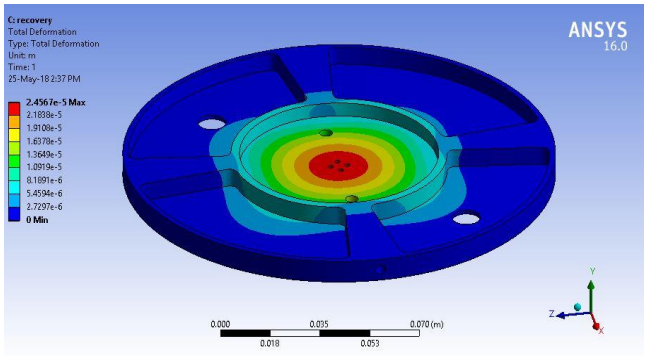


**Figure. Maximum deformation of the bulkhead.** The maximum deformation experienced by the bulkhead 0.025 mm.

### c) Analysis of shear stress on motor bay by the rail guide when rocket is mounted on rail guide

When the launch vehicle is mounted on the launch rail and made vertical, the entire weight of the rocket will act on the lower rail guide. This will lead to stresses on the fiberglass body and can be potentially lead to risks like launch lug tearouts. A method used to mitigate this effect is to add a reinforcement on the inner side of the fuselage to reduce stress on the mounted launch vehicle. We used an aluminium block epoxied to the fuselage on the inner side to which the launch lug was screwed in. This lead to reduction in stress on the body as shown below.

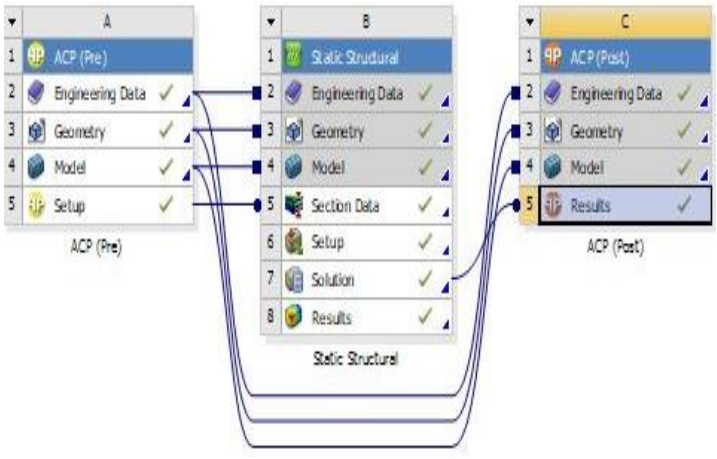


**Figure. Simulation tree for the analysis of stress on body**

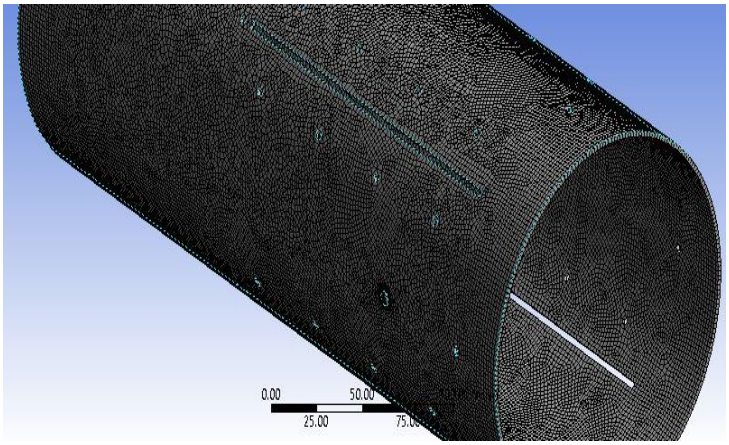


**Figure. Mesh for the body tube around the launch lug.** The motor bay has four 420 gsm layers of glass fiber.

Boundary Conditions- The following boundary conditions were applied:

i. A force equal to the weight of the assembled rocket was applied on the upper half of the hole.
ii. The top and bottom edges of the fuselage were fixed.

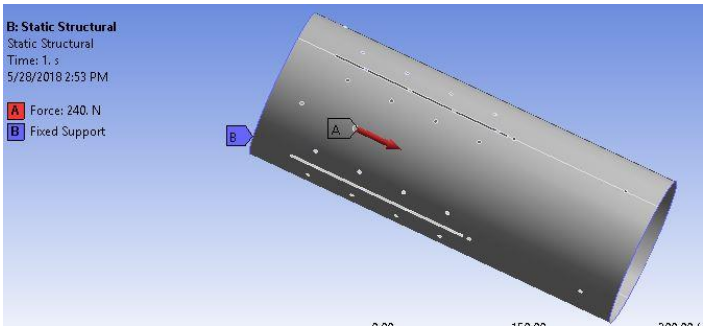


**Figure. Boundary conditions on the motor bay**

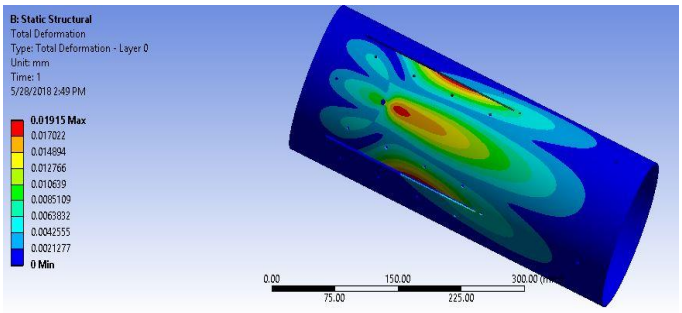


**Figure. Total deformation experienced by the fuselage due to the rail guide while resting on the launch rail.**

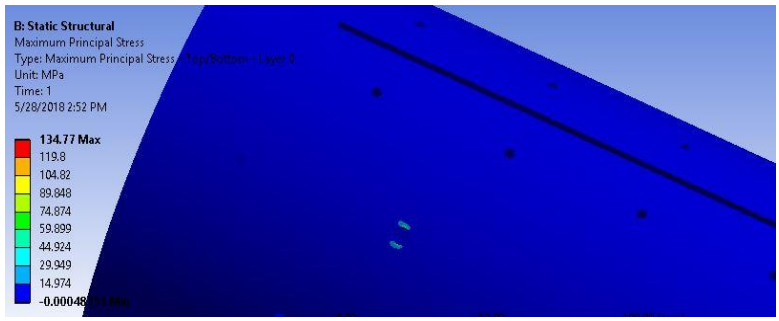


**Figure . The maximum principal stress acting in the vicinity of the hole.**

A stress of 135 MPa, although within safe limits, does not offer a factor of safety high enough to be safe for flight, so we added an aluminium block to reinforce this part and the results obtained were as follows:

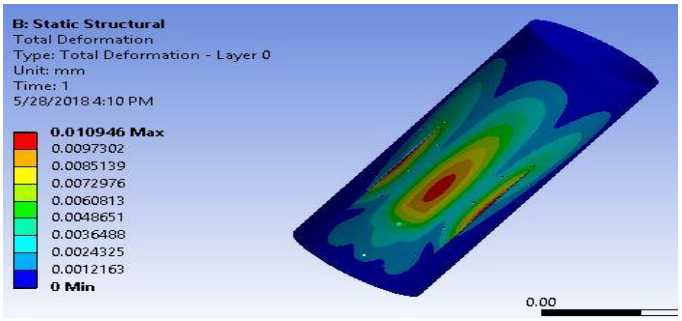


**Figure. Total deformation experienced by the fuselage after addition of aluminium block for reinforcement.**

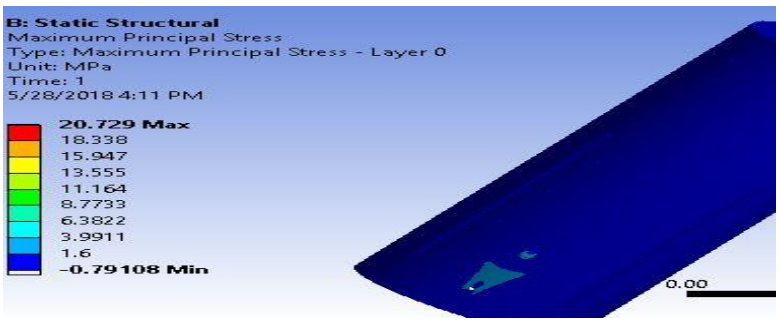


**Figure . The maximum principal stress acting in the vicinity of the hole after addition of aluminium block for reinforcement.**

As we can see, the stress reduces 6.5 times to about 21 MPa, which is safe for mounting rail guide on launch rail. There is also a 43% rduction in deformation in the fuselage body due to the rail guide fastener.

**d) Deformation and failure analysis of fin**

Based on the data of expected forces on the fins obtained from the aerodynamics team, we performed the structural analysis of the fins to check for structural failure of the fins during flight.

The fins were made by 6 layers of 420 GSM glass fiber. The motor bay with 4 layers of 420 GSM glass fiber. The boat tail with 1 layer of 100 GSM glass fiber, 2 layers of 200 GSM glass fiber and 4 layers of 420 GSM glass fiber.

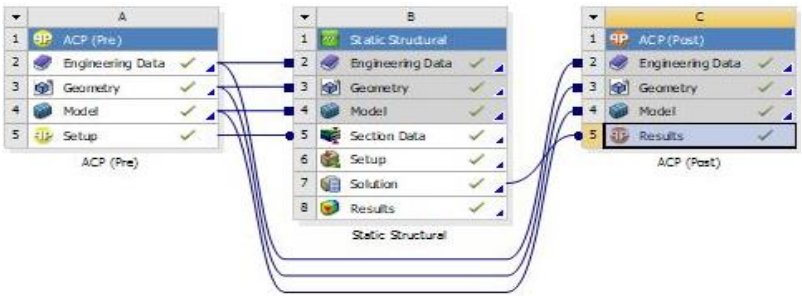


**Figure. Simulation tree for structural analysis of fins**

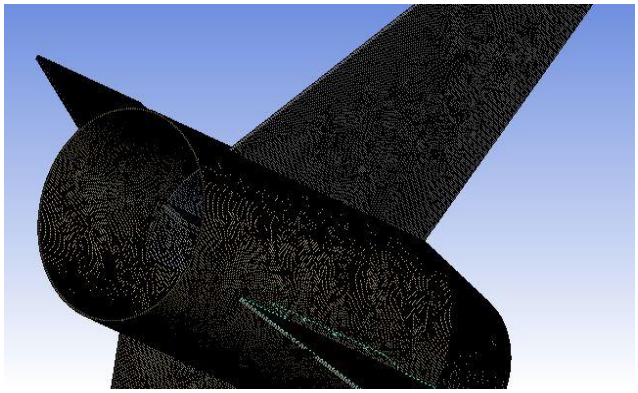

**Figure. Mesh of the fin fuselage assembly.**

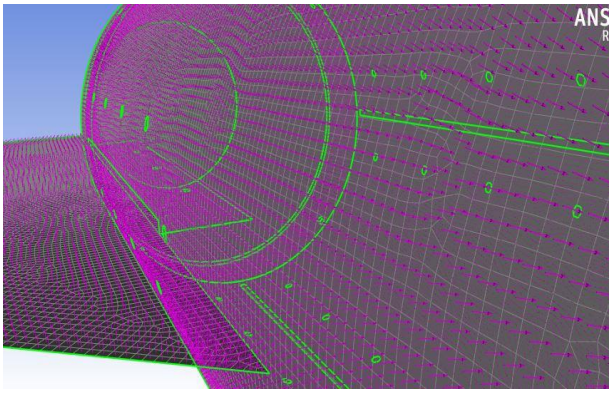

**Figure. Orientation of the fabric in the fin fuselage assembly.**

**Boundary Conditions**: The following boundary conditions were applied for analysis of the fin assembly.

i. Force: 45N on leading edge of fin and 15N on tip cord
ii. Fixed supports: Fastener holes of flanges, fastener holes of fin, fastener holes of boat tail and fuselage.

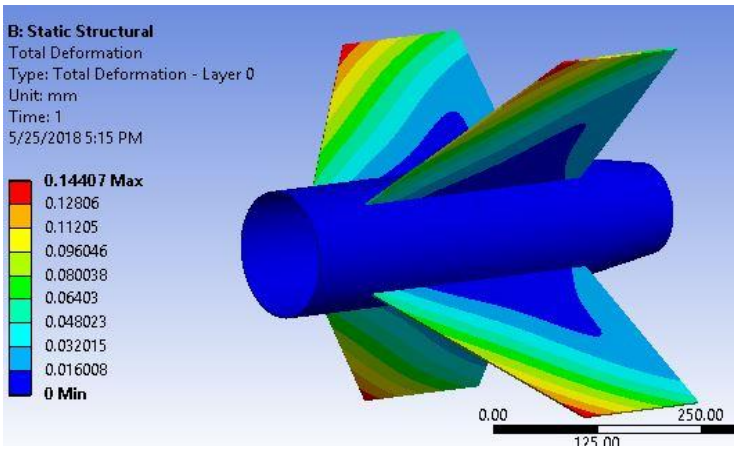


**Figure. Maximum deformation observed in fins.** Maximum deformation of 0.14 mm is observed.

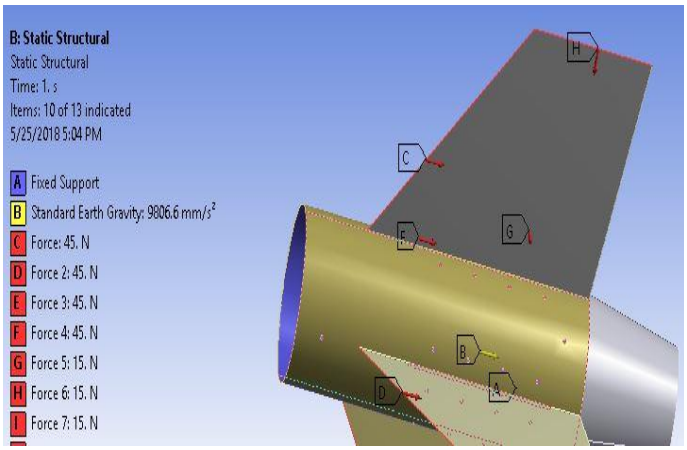


**Figure. Boundary conditions applied on the fin assembly**

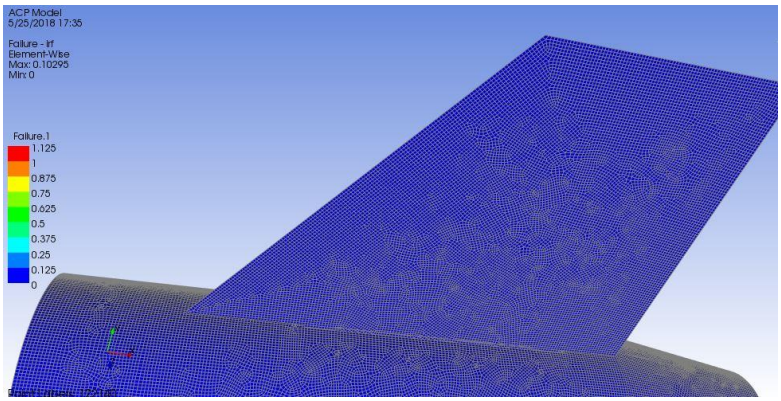


**Figure. ACP Post analysis.**

A magnitude of 1.125 in ACP (Post) means failure of the fiberglass body. We got results showing a magnitude of maximum 0.10295, meaning the fiberglass composite can handle the applied forces well enough to be flight ready.

**e) Analysis of payload bulkhead to check bulkhead strength against loads due to avionics mount**

The bulkhead supporting the TRON mount will also bear the load of the avionics components in addition to loads encountered due to thrust and acceleration of the rocket. The boundary conditions applied during analysis were as follows:

i. Fixed support applied to holes for fasteners.
ii. Weight of avionics bay mount and components applied to surface of bulkhead.
iii. Weight of the bulkhead itself.
iv. Maximum acceleration of the rocket.
v. Maximum thrust force.

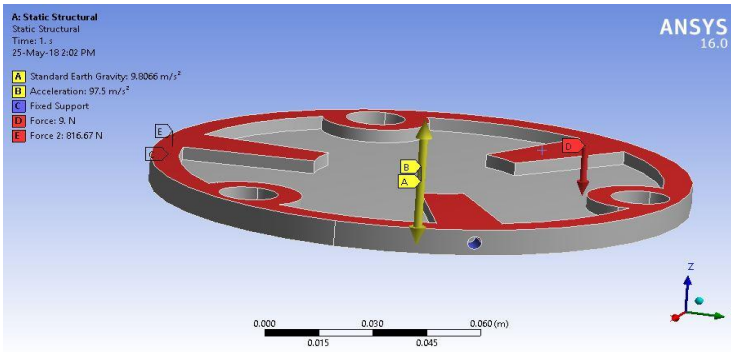


**Figure. Loads and supports applied to avionics bay bulkhead.**

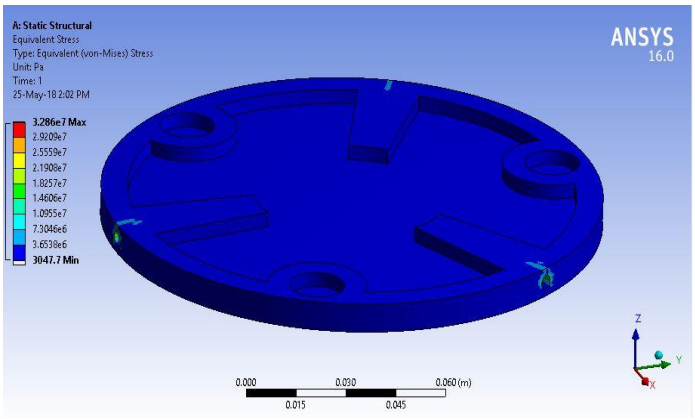


**Figure. Equivalent stress on the bulkhead.**

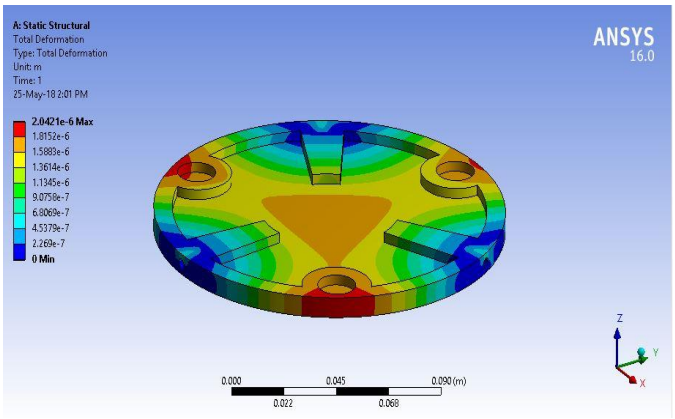


**Figure. Deformation experienced by the bulkhead.**

The maximum equivalent stress on the avionics bulkhead was 33 MPa, allowing a factor of safety of over 8 while the deformation was just over 2 micrometer, which is insignificant and can take taken to be safe and flight ready.

## D. Recovery Subsystem

The rocket shall be recovered by a single parachute acting as both the drogue parachute (in reefed condition) and main parachute (in unreefed condition).

### Setup

The parachute will be stuffed inside a parachute liner, with the liner used to protect the parachute from the flames and heat coming out of the pyro setup. The nosecone will be attached to the fuselage by four 2-56 nylon shear pins. At the other end, an aluminium container containing black powder would be mounted on the bulkhead and the bulkhead fastened on to the fuselage. The container would be covered by an aluminium piston. A nichrome igniter would pass from the other end of the bulkhead into the black powder. As the flight computer (or the backup stratologger) detects the apogee, current is sent into the igniter which causes the nichrom to het up and melt; this heat is enough to ignite the black powder. The black powder burns almost instantaneously, building up pressure in the container unltil it is high enough to push out the piston. When the piston is pushed out, it produces enough pressure to force the parachute out of the body, breaking the shear pins and pushing the nose cone out in the process.

### Recovery Parachute

### Canopy Shape:

The Nominal Diameter ($D_o$) of the parachute can be calculated from the total canopy surface area, $S_o$, including the area of the vent and all other openings. For descent, the recommended canopy shapes are flat circular and hemi-spherical,

Mass of the rocket after motor burnout = 19714 g

Note: All calculations are made using standard atmosphere values at sea level, as the descent velocity while touching the ground is important.

- To maintain a decent descent velocity (around 8 m/s) the skirt diameter should be nearly 230cm.
- Adding a spill hole (vent) reduces the $C_d$, so to compensate the drag loss, the skirt diameter can be increased to 240cm.

  Coefficient of Drag: For flat circular type the Cd is around 0.9.

  The area that needs to be considered while calculating the total drag is the nominal area or total canopy area (including the area of the vent).

| TYPE | CONSTRUCTED SHAPE PLAN | CONSTRUCTED SHAPE PROFILE | $\frac{D_c}{D_o}$ | INFLATED SHAPE $\frac{D_p}{D_o}$ | DRAG COEF $C_{D_o}$ RANGE | OPENING FORCE COEF $C_X$ (INF MASS) | AVERAGE ANGLE OF OSCILLATION, DEGREES | GENERAL APPLICATION |
|---|---|---|---|---|---|---|---|---|
| FLAT CIRCULAR | | | 1.00 | 0.67 TO 0.70 | 0.75 TO 0.80 | ~1.7 | ±10 TO ±40 | DESCENT, OBSOLETE |
| CONICAL | | | 0.93 TO 0.95 | 0.70 | 0.75 TO 0.90 | ~1.8 | ±10 TO ±30 | DESCENT, M < 0.5 |
| BICONICAL | | | 0.90 TO 0.95 | 0.70 | 0.75 TO 0.92 | ~1.8 | ±10 TO ±30 | DESCENT, M < 0.5 |
| TRICONICAL POLYCONICAL | | | 0.90 TO 0.95 | 0.70 | 0.80 TO 0.96 | ~1.8 | ±10 TO ±20 | DESCENT, M < 0.5 |
| EXTENDED SKIRT 10% FLAT | | $0.1\,D_c$ | 0.86 | 0.66 TO 0.70 | 0.78 TO 0.87 | ~1.4 | ±10 TO ±15 | DESCENT, M < 0.5 |
| EXTENDED SKIRT 14.3% FULL | | $0.143\,D_c$ | 0.81 TO 0.85 | 0.66 TO 0.70 | 0.75 TO 0.90 | ~1.4 | ±10 TO ±15 | DESCENT, M < 0.5 |
| HEMISPHERICAL | | | 0.71 | 0.66 | 0.62 TO 0.77 | ~1.6 | ±10 TO ±15 | DESCENT, M < 0.5, OBSOLETE |

**Figure. Solid Textile Parachute**

### Suspension lines:

However, the drag coefficient clearly increases with an increase in suspension-line ratio, $L_1/D_0$. The slopes of the curves for area and projected diameter growth indicate that using suspension-line ratios larger than 1.1 may have provided additional drag. Calculations indicate that line-length ratios above 1.5 may be detrimental because of the associated weight increase of the longer lines. For the canopy dimensions stated above the length of the suspension lines is 288cm (taking line ratio $L_o/D_o$ as 1.2).

### Parachute Deployment:

Parachute deployment denotes the sequence of events that begins with the opening of a parachute compartment or parachute pack attached to the body to be recovered. Deployment continues with extraction of the parachute until the canopy and suspension lines are stretched behind the body and the parachute canopy is ready to start the inflation process. This deployment is associated with a mass shock (snatch force) created by the acceleration of the mass of the parachute to the velocity of the body to be recovered. But in our case as the apogee is less the parachute is deployed quickly after attaining the maximum height. However a minimum time should be given for the rocket to gain enough speed for complete inflation of the parachute.

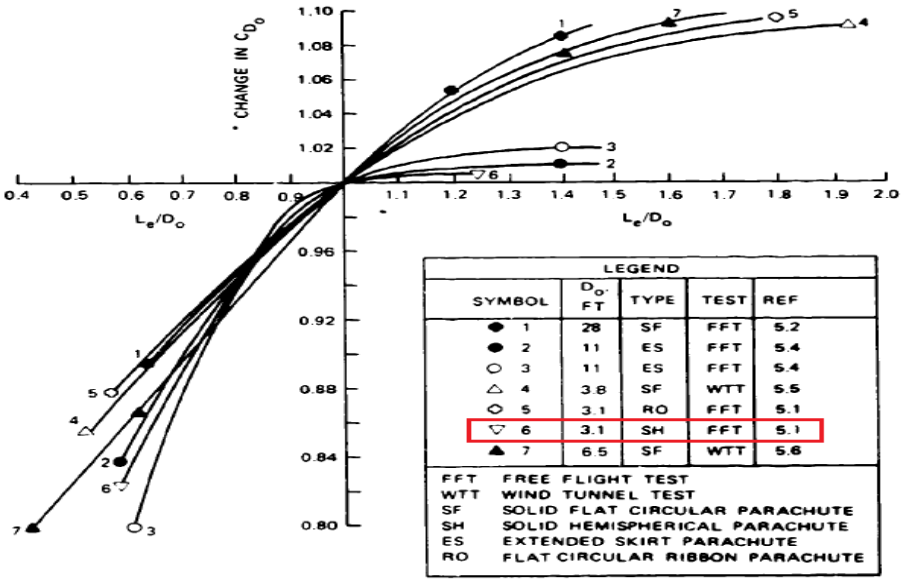


**Figure. Variation of drag coefficient with suspension-line ratio for several parachute types**

**Materials used:**

For canopy: Ripstop Nylon 42 GSM - Ripstop fabrics are woven fabrics, often made of nylon, using a special reinforcing technique that makes them resistant to tearing and ripping. During weaving, (thick) reinforcement threads are interwoven at regular intervals in a crosshatch pattern. The intervals are typically 5 to 8 millimeters (0.2 to 0.3 in). Thin and lightweight ripstop fabrics have a 3-dimensional structure due to the thicker threads being interwoven in thinner cloth.

Paracords: 7 strand Nylon paracords - These paracords come with a nylon outer sleeve to protect them from mechanical abrasion.

**Reefing Parachute**

A reefed parachute is one in which the canopy opening is constricted to reduce drag production. This is done by rigging a cord around the periphery to reduce canopy volume. When an increase in drag is needed, the cord is cut allowing full canopy deployment.

This is needed to serve the following purposes:

- Reduce the parachute opening forces to a pre-determined value through successive steps of parachute opening.
- Increase the parachute stability & reduce the opening snatch force.
- Reefing the parachute to a low drag area permits a more accurate drop from high altitude and obtain a temporarily high rate of descent. Low-impact velocity is then obtained by dis-reefing the parachute shortly before ground impact.

Reefing rings are attached to the canopy skirt inside of the canopy at the connection point of each suspension line. The reefing line is a continuous line that restricts the opening of the canopy and is guided through the reefing rings and several reefing-line cutters. Each cutter contains a pyro-time train and a cutter knife and is initiated at canopy stretch by pull cords attached to the suspension lines or to the canopy. After a preselected time, the cutter fires and the knife severs the reefing line, allowing the canopy to open fully. The length of the reefing line is determined by the required reduction in parachute drag area, called reefing ratio. The reefing-line ratio is defined as the ratio of the reefing-line circle diameter to the nominal diameter of the parachute.

**Parachute Simulations:**

Four ellipsoidal parachutes having different b/a ratios are analysed under same physical conditions of pressure, velocity and temperature. The inlet velocity is taken as 20 m/s in the positive y direction at 1 atm pressure and 293.2 K. Here ‘b’ refers to the canopy height and ‘a’ is the base radius of the open parachute.

We ran some simulations to decide the canopy shape of our parachute using solidworks.

The following are the pressure contours on the surface of the canopies:

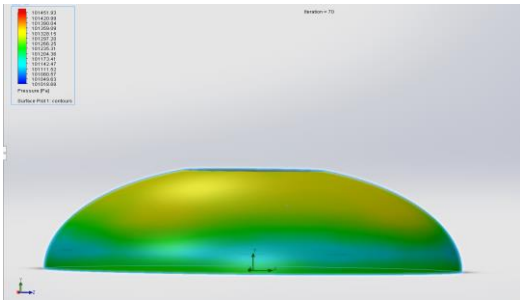

**Figure. Pressure contour for b/a = 0.6**

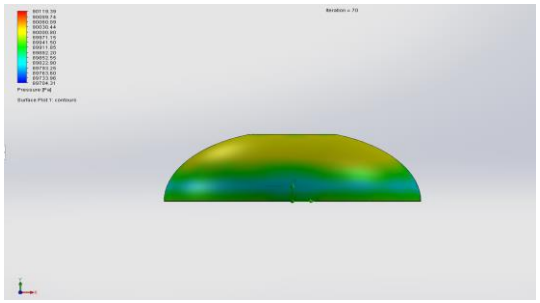

**Figure. Pressure contour for b/a = 0.7**

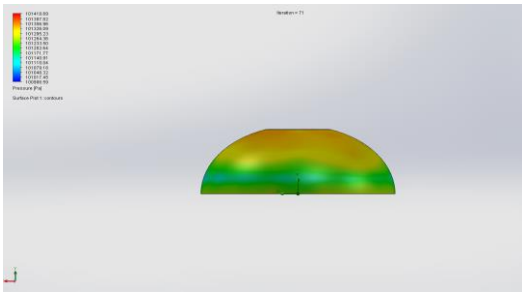

**Figure. Pressure contour for b/a = 0.8**

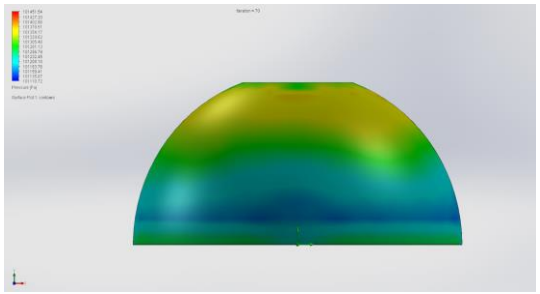

**Figure. Pressure contour for b/a = 1**

It is observed that high pressure distribution covers more area in case of parachutes with b/a ratios 0.6 and 0.7 respectively. It is a desirable factor in a canopy so that there isn't any stress concentration and the material doesn't fail.

**Construction**:

The recovery system in our rocket is a single parachute dual sequence deployment. To accomplish this objective, we will be using a ten gore skirt reefed elliptical canopy parachute of projected diameter 240cm where the ratio of height to radius is 0.707. The rocket will achieve an ultimate terminal velocity of 8m/s.

A parachute with an elliptical canopy has essentially the same $C_d$ as a hemispherical parachute or a parasheet of the same deployed diameter but uses less material in the assembled parachute than the hemispherical or parasheet type and as a result should be a little lighter than the parasheet type of equivalent diameter.

To form a parachute that deploys as a semi-ellipsoid, we take the desired three dimensional semi-ellipsoidal shape and divide it into a number of two dimensional panels, called gores. Each gore is individually cut to a specific shape so that when re-assembled it will form a semi-ellipsoid upon deployment.

This particular parachute is comprised of 10 *gores*, or panels, individually cut from the fabric material, and sewn together to form the canopy. The shape of the gores was calculated and was generated using MATLAB to achieve a height to radius ratio of 0.707. Here are the MATLAB code and the plot of the gore:

```
clc
clear all
close all
%constructed diameter
D=240;
%ellipse
a = D/2;
b = a*0.707;
= 648.273/4;
%no of panels
n = 10
%Panel angle
fi = (2*pi)/n;
th = linspace(pi/2,0,100);
r_sec = a* cos(th);
y = 0.5*fi*r_sec;
d = l-b*ellipticE(atan(a/b*tan(th)),1-(a/b)^2);
plot(d,y); hold on; plot(d, -y);
```

**Figure. MATLAB code of gore**

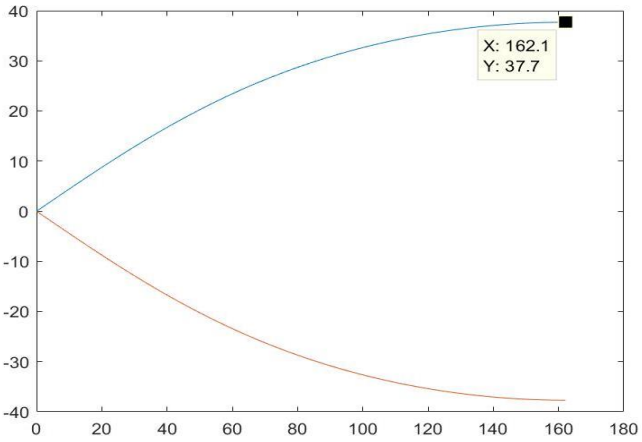


**Figure. Plot of the gore**

The above pattern was then traced out on the fabric and hemmed along both curved edges and along bottom edge. Ten such patterns were produced. The panels were then joined using seam binding. Four such lengths of seam binding, long enough to span the entire arc length of the canopy were used.

Reefing was chosen over dual deployment because of the following reasons:

- Reduction of mass as we used only one parachute instead of two.
- The deployment sequence was less complicated in both mechanical and electronics aspects as less number of components were used. Also instead of splitting the rocket into three components, it was split in only two.
- Since only one parachute is used, it occupies less space.

**Drag Reduction in Reefing Parachutes**

When un-reefed, the canopy opening is about 30 - 60% of the skirt diameter. The drag coefficient for a typical un-reefed flat circular parachute is on the nominal diameter.

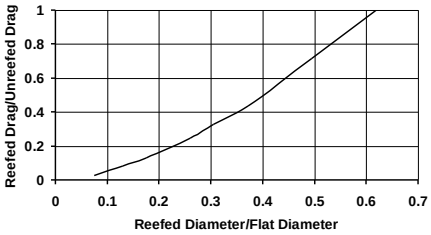


**Figure. Drag of reefed flat circular parachutes**

**Reefing Line Attachment**

While there are multiple techniques, the key issue is friction between the reefing line and its attachments to the canopy. With too much friction, full deployment when the reefing line is cut can be significantly impaired. The reference suggests that a metal reefing line ring be sewn to the canopy edge between each pair of suspension lines. Thus, if there are 10 suspension lines, the reefing cord would pass through 10 rings.

**Dis-Reefing**

The process of restoring a reefed parachute to its full, unrestricted diameter is called dis-reefing. It is often accomplished with a piston-type pyro-cutter. The line to be cut passes transversely through the cylinder, and a black powder charge drives a piston down the cylinder where the line is sheared in two places. The only trick here is that ordinary nylon parachute cord is tough to shear. Attaching the reefing cord to a solid nylon strip used for forming wires into bundles will solve this problem.

**Testing**

**Static Pressure Ports:**

**Aim**: To check for pressure equilibrium between the airframe and the atmosphere (crucial for avionics operations and structurally reduce pressure stress on the airframe).

- Inflight airflow replicated inside an open loop sub-sonic wind tunnel.
- A section of the airframe (with nosecone) was placed in the test section with the help of a custom built wind tunnel mount.
- The quick pressure balance achieved in the airframe (recognised by the on-board sensors which are monitored from outside) marked the success of the test.

**Pressure Sensor Calibration:**

**Aim**: Calibrate the pressure sensors (gauge & differential) procured (as most of them were analogue and required calibration).

- All the sensors are calibrated against U-tube manometers connected to the wind-tunnel.
- A pitot tube is used for differential pressure calibration.

**Parachute Reefing Test:**

**Aim:** To test dual sequence single parachute recovery.

- Ram air is provided by tugging the system behind a puck-up truck.
- Several design problems were cleared with this testing.
- The canopy was stable, no canopy spin (in both reefed/un-reefed conditions), no damage to pyro-cutter wiring
- Un-reefing sequence was tested multiple times and was successful.

**E. Payload**

The rules of the competition require the launch vehicle to carry a payload of a minimum weight of 4 kg. For this purpose, the team will be making use of a non-functional payload. The payload itself is a 3U CubeSat, to which dead weight has been added to meet the minimum weight requirement.

**a)** **b)** **c)**

**d)** **e)**

**Figure. CAD model and actual 3U CubeSat payload.** Figure a) is the base plate. Figure b) is the supporting rod. Figure c) is the support plate. Figure d) is the assembled model of a 2U CubeSat. Figure e) is the actual CubeSat.

**The Design**

The CubeSat consists of an aluminium frame enclosed in fiber-glass laminates that have been fastened on to the frame. The frame consists of aluminum rods and square base plates fastened using M3-16 screws. The rods have an extrusion at one end and a pocket at the other such that the extrusion of one rod slides into the pocket of the other, thus making it easier to assemble.

All of these components were machined using a Vertical Milling Center. The square holes in the rod were cut using Wire EDMs. The material used for these is aluminium 6061 TS.

When completely assembled, the 3U CubeSat along with the fiberglass panels weighs about 910g. The remaining weight is added by machining a mild steel rod to the required dimensions and securing it with in the CubeSat.

**Structural Analysis**

Structural analysis of the design was performed by the ANSYS Static Structural solver. The individual components were modelled as being bonded. A weight of 30N was applied on each plate. Hence a total weight of 90N (factor of safety over 2) was simulated. We took into account the highest acceleration achieved before motor burnout. The maximum expected acceleration of the rocket is 97.5 m/s$^2$. We considered a factor of safety of about 2.

**Results**

The total deformation and the equivalent stress (von-mises) were calculated.

Maximum deformation of 0.016 mm was estimated.

Maximum equivalent stress of 3.93 MPa was estimated.

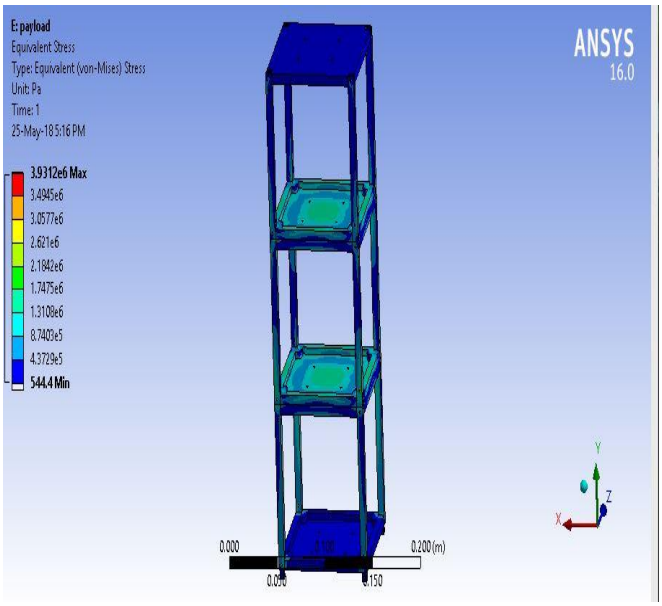


**Figure. Equivalent stress on payload structure.** The stress was within limits hence design is safe.

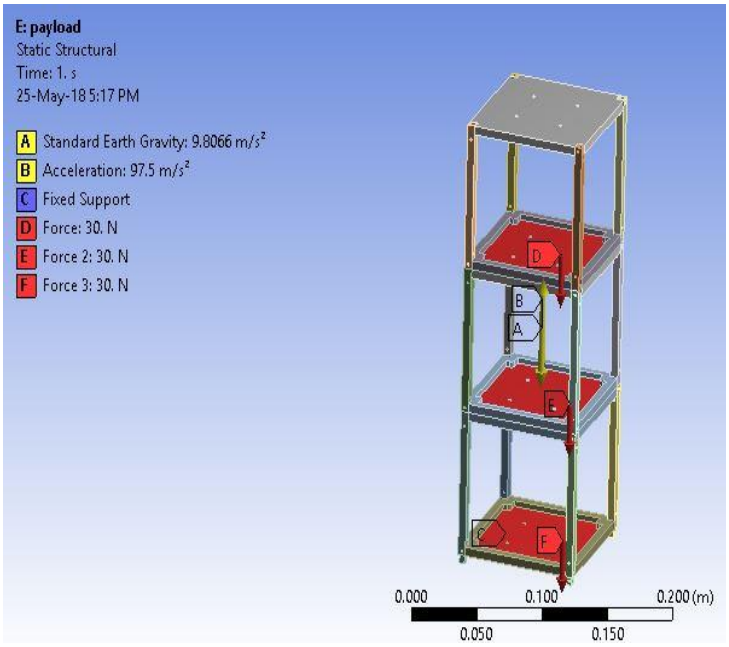


**Figure. Boundary conditions applied on the payload structure.** The base plate has been fixed and acceleration of 97.5 m/s$^2$ was applied based on expected flight performance. The weight was applied and 90N force was equally divided among the three compartments as a multiple of the installed dead weight for factor of safety.

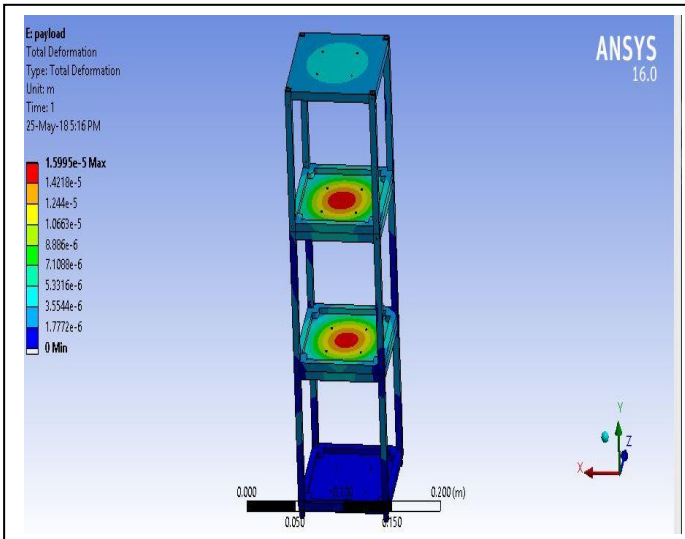


**Figure. Deformation experienced by payload structure**

## III. Fin Flutter Analysis

Aeroelasticity deals with elastic body-fluid interactions and the effect of aerodynamic forces when a body is subjected to fluid flow.

To study the effects of aeroelasticity on fins while in flight, we conducted experiments on a fin prototype (a square composite laminate). The main aim of the tests was to check if the deformation was under permissible limit. The same setup was then simulated in ANSYS by applying a suitable project scheme in the workbench.

**Wind tunnel tests**

The 146 mm x 122 mm laminate was made of 2 mm thick E grade fiberglass. The test was carried out in a wind tunnel at a wind speed of about 30 m/s. An accelerometer was attached at the back of the fin to measure deflections in either direction. The experimental setup was arranged such that the air would flow across the fin to measure maximum deflection to mimic gusts of wind at higher altitudes.

**Figure. Wind tunnel setup for flutter**

The data received from the accelerometer at varying wind speeds was filtered and the output received was in angle. This was then converted to deflection in mm using suitable assumptions (it was assumed that the fin acts as a cantilever beam). The results obtained from the accelerometer were:-

| RPM | Deflection in degrees | deflection in mm |
|---|---|---|
| 900 | 1.81 | 3.79 |
| 800 | 1.39 | 2.91 |
| 700 | 1.1 | 2.30 |
| 600 | 0.84 | 1.76 |
| 500 | 0.53 | 1.11 |
| 400 | 0.32 | 0.67 |
| 300 | 0.12 | 0.25 |
| 100 | -0.01 | -0.02 |
| 0 | 0 | 0.00 |

**Figure. Fin deflection due to wind speed (based on RPM of fan)**

To replicate this scenario in ANSYS, a schematic was created in the ANSYS workbench and simulations were performed. There were various paths created, the one selected is shown below.

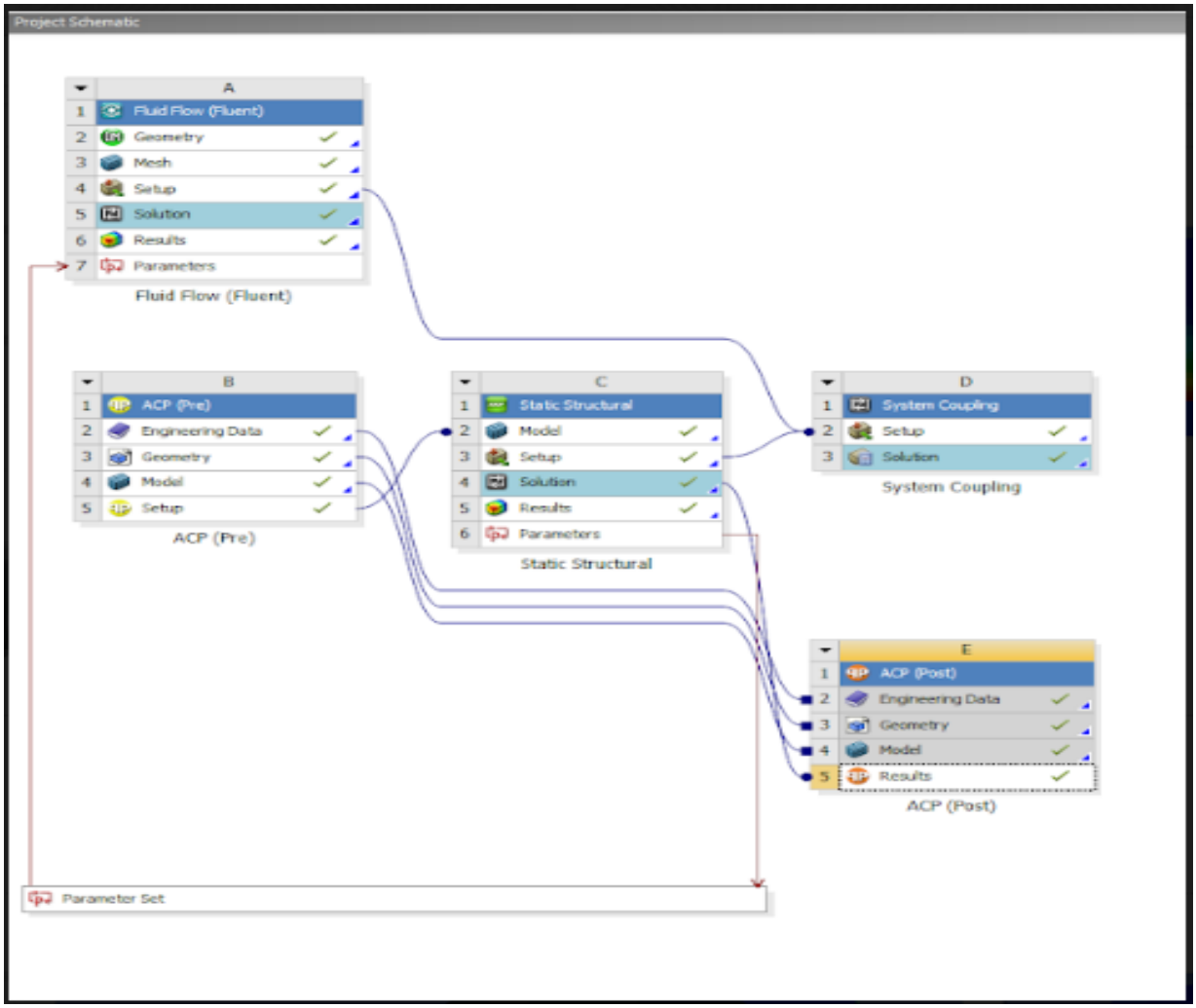


**Figure. Schematic to validate wind tunnel tests**

The schematic above represents a Fluid-Structure Interaction (FSI) along with composite modelling. The solvers used for the FSI were Ansys Fluent and Static Structural. The two were coupled using the System Coupling Solver of Ansys. Composite Modelling was done using the ACP (pre) and ACP (post). A parameter set was defined in order to obtain the maximum deflections at different velocities.

The flow is modelled as a pressure based, steady, incompressible flow. The k-epsilon turbulence model was used. The pressure data from fluent is transferred to static structural in real time where the deformation due to that pressure is calculated and accordingly the mesh in fluent is updated with these deformations. The structural solver also gets input from the ACP (pre) which allows it to take into account the composite properties. The mechanical data regarding the composite (as shown below) is then collected from ACP (Post). The highest in-plane stress was found to be 1.42 Mpa which was well below the critical level. The maximum deformation was found to be 2.07mm at a wind speed of 32 m/s. Hence the result from the simulation was in a comparable range with the actual wind tunnel test.

A graph was plotted for deflection in the fin at various flow velocities.

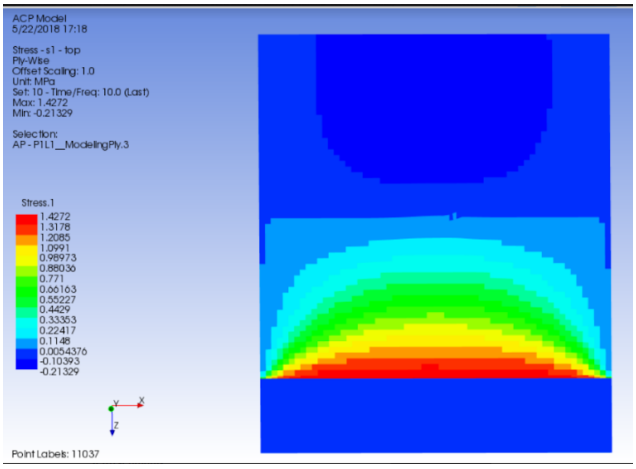


**Figure. Maximum in-plane stress**

The figure below confirms that, in-plane failure is not observed and is well within the safe limit. If the value would have crossed 1.125 it would have then indicated failure in the ply.

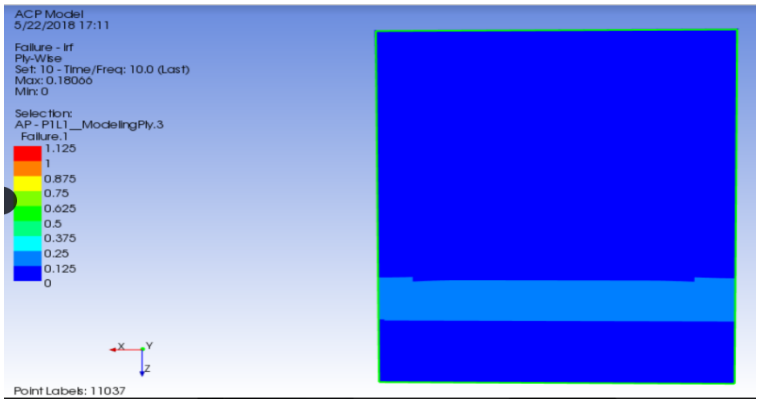


**Figure. Region of probable failure in fin**

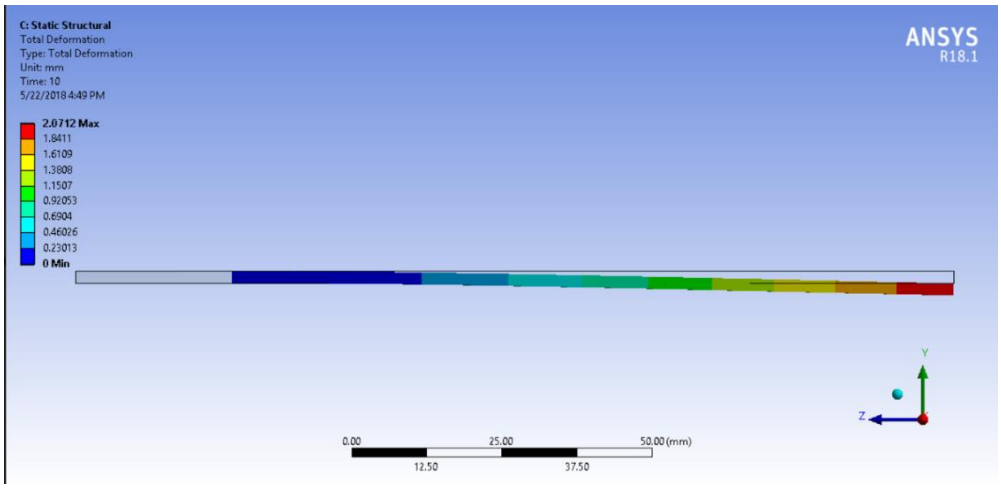


**Figure. Deformation experienced by the fin along the length**

**Comparison**

The maximum deformation from the simulation was estimated to be 2.07 mm. Actual wind tunnel tests showed deformation of 3.79 mm. Comparison of deformation vs speed data from the actual test and the simulation is shown below. From this analysis, we can conclude that some minute error would be there in the analysis of the actual launch vehicle fin. The variation in result can also be attributed to the error in the readings given by the accelerometer and the variation in the ratio of the resin and hardeners used by the manufacturing team, because ANSYS takes the ideal case i.e. a uniform mixture of resin, while solving ACP. These are the major factors responsible for the variation in the theoretical result and experimental setup. We are working towards improving the accuracy of our sensors and also looking for better sensors to measure this deflection. We are trying to avoid variations due to setting time and proportions of resin and hardeners.

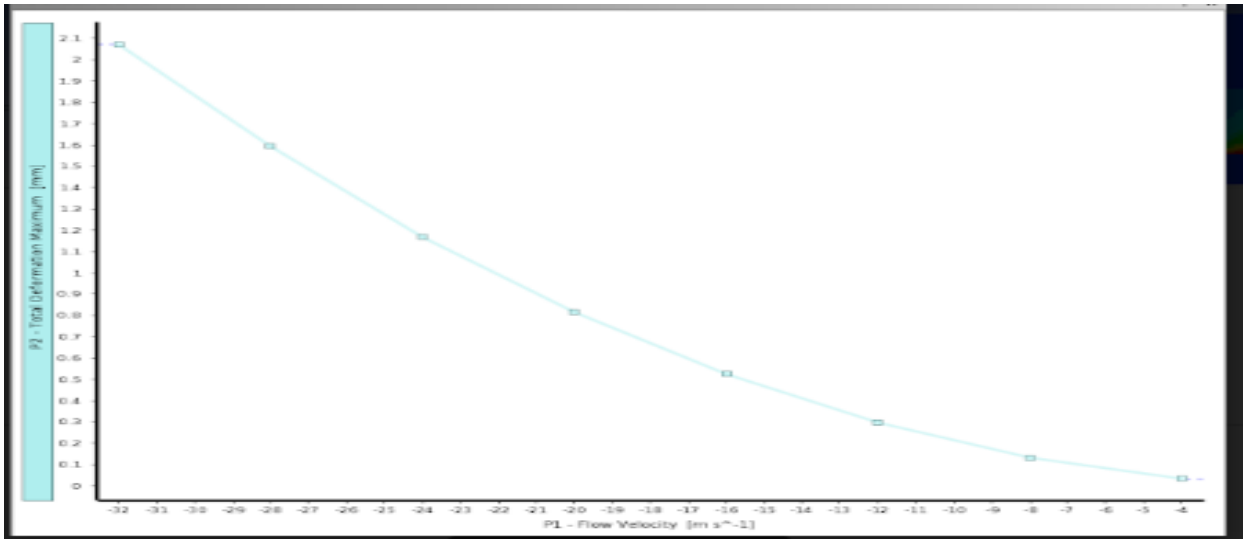


**Figure. Graph obtained from ANSYS simulation**

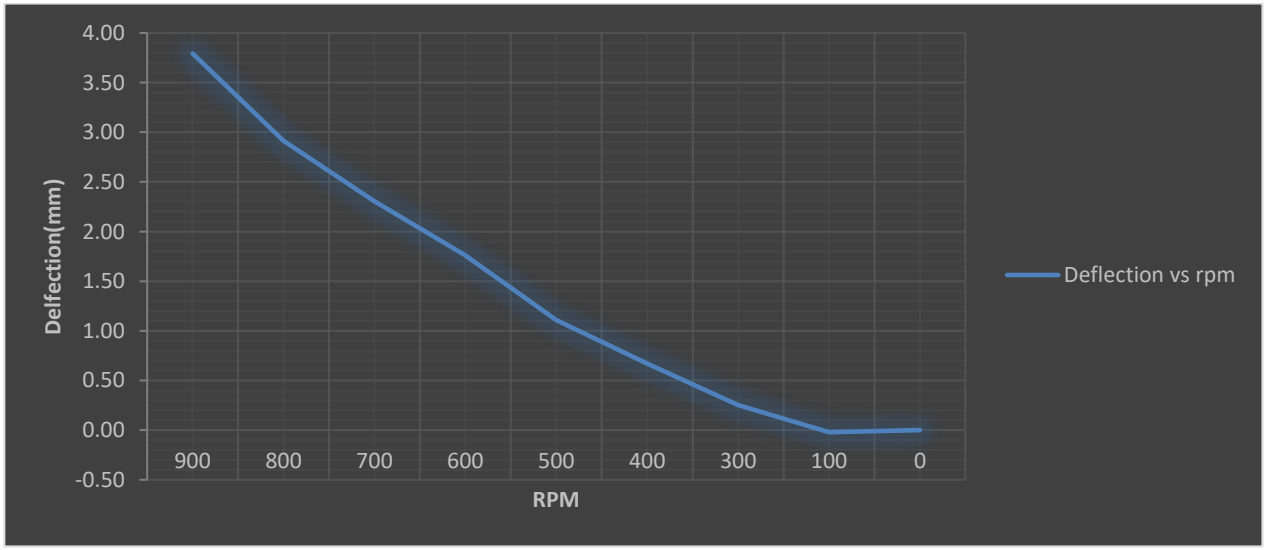


**Figure. Actual graph obtained from wind tunnel test**

## IV. Mission Concept of Operations (CONOPS) Overview

## V. Conclusion and Lessons Learned

Beginning a rocketry club in India, where rocketry at a student level is virtually unheard of, came with its own set of challenges. From skepticism regarding the feasibility of our project to unavailability of rocketry related products domestically, we have faced it all. However, with continued support from our university, our families, our sponsors who trusted us with their products as well as the rocketry communities based in the USA, who helped us when we faced unexpected problems, we overcame these challenges, learning a lot in the process, not just rocketry jargon or technicalities of the science, but also management practices.

Many members of the team learnt the use of various tools and devices which were otherwise not accessible in the classroom. The hands on experience gained by the members will be cherished. Moreover, the qualities of team-work, time management, project management and problem solving that have been inculcated in the team members during the course of the project would help us in our careers as well.

The team members in the mechanical division learnt softwares such as CATIA, SolidWorks and ANSYS for design and analysis, equipping them with skills relevant to the industry.

Since this was our first time, the manufacturing division of the team got their hands on glass fiber composite manufacturing for the first time, and while manufacturing, they learnt about the various manufacturing techniques, improvement of composite as well as surface finish techniques to get the best products. Towards the end, we noticed getting some in house manufactured components better in quality than commercially available ones!

From the management perspective, we learnt about the various formal procedures employed while executing something of this scale, especially the administrative delays and paperwork dealt with during the process.

As the seniors leave the team after the competition, they have taken various measures for smooth transition of the team to the juniors, for example, they have transferred over all the intelligence learnt during their time in the team through reports and briefings. Moreover, during testing, a junior who was expected to look at the proceedings carefully and then replicate the tests for better understanding.

This way, the team looks forward to more ambitious rockets coming out in the next few years.

## Appendix I

An appendix, if needed, should appear before the acknowledgements.

## Appendix II

## Appendix III

## Appendix IV

## Appendix V

## Appendix VI


## Acknowledgments

We would like to thank our university, Manipal Academy of Higher Education, for helping us start the project, providing financial support as well as access to facilities like the sub-sonic wind tunnel for carrying out our tests. We also thank our faculty advisor, Mr. Srinivas G. for providing us with resources whenever required and keeping the team members motivated throughout the journey.

We would like to thank our sponsors:

- Atul
- Polymer Products of India
- CFW Enterprises
- ANSYS
- SolidWorks
- Sanjay Group

- Babaji Shivram

We also thank our friends in the university for keeping us enthusiastic about our project by badgering us with questions about our progress with our rockets.

And most importantly, all students involved with the project would like to thank their families for maintaining faith in them and supporting them when they felt unsure about themselves.